Antiproliferative and bactericidal activity of diiron and monoiron cyclopentadienyl carbonyl complexes comprising a vinyl-aminoalkylidene unit

Antiproliferative and Bactericidal Activity of Diiron and Monoiron Cyclopentadienyl Carbonyl Complexes Comprising a Vinyl-Aminoalkylidene Unit

Dalila Rocco [a,§,#], Natalia Busto,[b,#] Cristina Pérez-Arnaiz,[b] Lorenzo Biancalana,[a] Stefano Zacchini,[c] Guido Pampaloni,[a] Begoña Garcia,[b*] Fabio Marchetti [a,*]

[a] *Università di Pisa, Dipartimento di Chimica e Chimica Industriale, Via G. Moruzzi 13, I-56124 Pisa, Italy.*

[b] *Universidad de Burgos, Departamento de Química, Plaza Misael Bañuelos s/n, 09001 Burgos, Spain.*

[c] *Dipartimento di Chimica Industriale "Toso Montanari", Università di Bologna, Viale Risorgimento 4, I-40136 Bologna, Italy.*

Corresponding Authors

*E-mail addresses: fabio.marchetti1974@unipi.it; begar@ubu.es.

[#]These authors equally contributed to the work. [§]Present address: Department of Chemistry, University of Basel, BPR 1096, Mattenstrasse 24a, CH-4058 Basel, Switzerland.

Abstract

A series of diiron complexes with two cyclopentadienyls, two carbonyls and one bridging vinyl-aminoalkylidene as ligands, [**3a-h**]CF_3SO_3 and [**4a-d**]CF_3SO_3, was synthesized in 66-94% yields from diiron μ-aminocarbyne precursors. The subsequent reactions with pyrrolidine led to selective fragmentation to aminoalkylidene-ferracyclopentenone derivatives, **5a-h** and **6a-c**, in 30-84% yields. The compounds were characterized by elemental analysis, IR and NMR spectroscopy, and by single crystal X-ray diffraction in three cases. The in vitro antiproliferative activity of the compounds was determined towards cancer (A2780, A2780cisR) and non cancer (HEK-293) cell lines; moreover, the antibacterial activity was tested on Gram-positive (vancomycin-resistant *E. faecium* and methicillin-resistant *S. aureus*) and Gram-negative strains (*A. baumannii* and *P. aeruginosa*).

Keywords: diiron complexes; iron-carbonyl complexes; bioorganometallic chemistry; amino-alkylidene ligand; cytotoxic and antibacterial activity.

Introduction

The synthetic design and development of new iron-based drugs represents an issue of current great interest, due to the unique properties of such metal element, being substantially nontoxic in many forms.[1] Thus, a variety of mono- [2,3] and diiron [4] carbonyl complexes has been investigated as CO-releasing agents, in view of the promising therapeutic profiles associated to a controlled administration of carbon monoxide.[5] Instead, a limited number of iron-carbonyl compounds has been evaluated for their anticancer behaviour in vitro;[6] on the other hand, following the discovery of the medicinal potential of the ferrocene skeleton,[7] several studies in this field have been focused on monoiron-cyclopentadienyl complexes, called piano-stool complexes. In fact, several piano stool complexes has been found to display strong cytotoxic activity against various cancer cell lines.[8] It should be expected that the combined introduction of both Cp (Cp = η^5-C_5H_5) and CO ligands on an iron centre may provide a synergic effect, resulting in a possible multi-therapeutic action and also improved chemical stability of the complex, due to the complementary electronic effects of the two ligands.[9] Nevertheless, mixed cyclopentadienyl-carbonyl iron compounds have been limitedly explored in medicinal chemistry so far.[10] In particular, the investigation on diiron structures still remains in its infancy,[11] although on the other hand diverse diiron carbonyl complexes have aroused a great attention in the recent years as biomimetic catalysts.[12]

The most convenient starting material for accessing both di- and monoiron complexes bearing Cp and CO ligands is the commercial dimer $Fe_2Cp_2(CO)_4$. This chemical represents a highly versatile scaffold to build functionalized bridging ligands, exploiting reaction routes which are commonly unavailable to mono-metal species, thanks to the cooperative effects supplied by the two bonded iron centres.[13,14] Piano-stool carbonyl mononuclear derivatives are obtained via fragmentation of $Fe_2Cp_2(CO)_4$, being promoted by oxidative 2[a,15] and reductive pathways,[16] or addition of suitable donors.[17]

Recently, we reported a preliminary study on the anticancer potential of diiron complexes with a bridging C_3 ligand supported on the $[Fe_2Cp_2(CO)_2]$ frame,[18] alternatively described as vinyliminium or vinyl-aminoalkylidene (Figure 1a).[19] Such complexes are available through a straightforward multigram procedure, and possess some promising drug-like properties, such as a balanced amphiphilicity and a substantial inertness in aqueous media. The complexes exhibited a variable antiproliferative activity against A2780 and A2780-cisR cancer cell lines, with some of them displaying IC_{50} values in the nanomolar range, and an appreciable selectivity compared to the non-tumoral HEK-293 cell line.[18] The cytotoxicity seems imputable to ROS production, other than possible weak DNA binding. Cationic diiron μ-vinyl-aminoalkylidene complexes are susceptible of a clean fragmentation by reaction with a reducing agent, such as sodium hydride [20] and cobaltocene,[18,21] affording neutral piano-stool monoiron complexes incorporating the intact vinyl-aminoalkylidene moiety (Figure 1b). On considering that the conversion into monoiron species may be triggered also by mild reductants, e.g. cyanide [22] and amines,[23] it has been hypothesized that this reaction is viable in a biological environment, contributing to the observed cytotoxicity of the diiron precursors. Indeed, some monoiron compounds display a moderate cytotoxicity, mainly attributed to ROS production, and especially those bearing a phenyl substituent on the vinyl moiety (R' = Ph in Figure 1a) are substantially nontoxic towards non tumoral HEK-293 cells.[18,23]

In the present paper, we will describe the synthesis of a series of diiron and monoiron cyclopentadienyl complexes containing carbonyl and vinyl-aminoalkylidene ligands, which have been assessed for their antiproliferative activity. On considering the paucity of data in the literature on effective bactericidal iron compounds,[24] the complexes have also undergone a preliminary investigation in this regard.

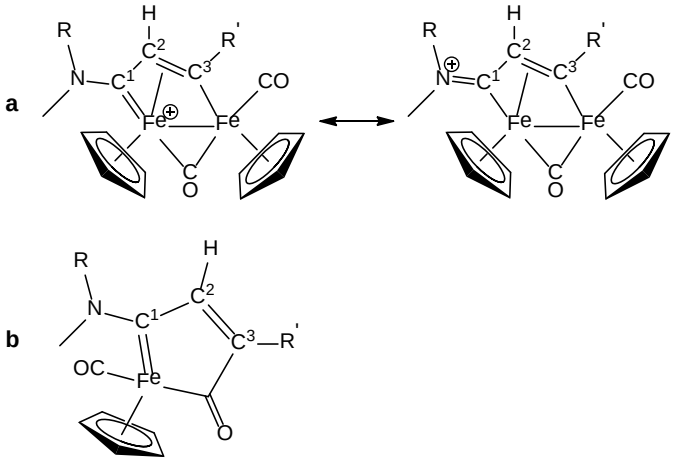

Figure 1. a) Diiron bis-carbonyl bis-cyclopentadienyl complexes with a bridging C_3 ligand alternatively described as vinyliminium and vinyl-aminoalkylidene (R = Me or aryl, R' = alkyl, aryl or other). **b**) Piano-stool iron carbonyl derivatives incorporating the vinyl-aminoalkylidene fragment.

Results and discussion

1. Synthesis and characterization of compounds.

The μ-vinyl-alkylidene compounds [**3-4**]CF_3SO_3, differing in the nature of the aryl group bound to C^3, were synthesized starting from the aminocarbyne precursors [**1-2**]CF_3SO_3, which in turn can be easily obtained in a multigram scale from the commercial $Fe_2Cp_2(CO)_4$ (Scheme 1).[25] The two step synthesis of [**3-4**]CF_3SO_3 consists in removal of one carbon monoxide, followed by insertion of aryl-acetylene into the iron-carbyne bond, with acetonitrile playing the role of labile ligand. The products were purified by alumina chromatography and finally isolated in 62-94% yields.

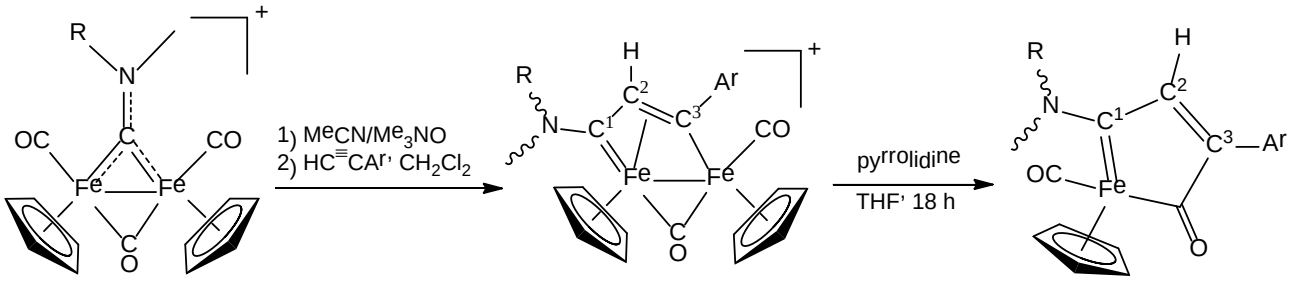

[**1**]$^+$ (R = Xyl)
[**2**]$^+$ (R = Me)

	R	*Ar*	
[**3a**]$^+$	Xyl	4-C_6H_4F	**5a**
[**3b**]$^+$	Xyl	3-C_6H_4F	**5b**
[**3c**]$^+$	Xyl	2-C_6H_4F	**5c**
[**3d**]$^+$	Xyl	4-C_6H_4Me	**5d**
[**3e**]$^+$	Xyl	3-C_6H_4Me	**5e**
[**3f**]$^+$	Xyl	4-C_6H_4Ph	**5f**

[**3g**]$^+$	Xyl	2-$C_6H_4NH_2$	**5g**
[**3h**]$^+$	Xyl	3-C_6H_4OH	**5h**
[**4a**]$^+$	Me	4-C_6H_4F	**6a**
[**4b**]$^+$	Me	2-$C_6H_4NH_2$	**6b**
[**4c**]$^+$	Me	3,5-$C_6H_3(CF_3)_2$	**6c**
[**4d**]$^+$	Me	4-C_6H_4Me	

Scheme 1. Synthesis of diiron μ-vinyl-aminoalkylidene complexes from aminocarbyne precursors (triflate salts), and subsequent fragmentation into monoiron complexes. Xyl = 2,6-$C_6H_3Me_2$.

Compounds [**3d,h**]CF_3SO_3 [19a,18] and [**4c,d**]CF_3SO_3 [23,19a] were previously reported, while the remaining eight products are new and have been fully characterized by IR and multinuclear NMR spectroscopy. In general, the IR spectra of [**3a-h**]CF_3SO_3 and [**4a-d**]CF_3SO_3 (in CH_2Cl_2) display a typical pattern made of two carbonyl absorptions and one less intense band ascribable to the C^2C^1N moiety, based on previous calculations on similar systems.[19c] The wavenumber of the terminal carbonyl absorption is influenced by the nature and the position of the Ar substituent. Thus, such absorption appears at 2010 cm^{-1} in [**3c**]CF_3SO_3 (substituent: ortho-F) and at 1992 cm^{-1} in the case of [**3g**]CF_3SO_3 (substituent: ortho-NH_2); a significant shift is observed also on going from [**3c**]CF_3SO_3 to [**3a**]CF_3SO_3 ($\tilde{\upsilon}$ = 2003 cm^{-1}, substituent: para -F). The C^2C^1N infrared band falls around 1630 cm^{-1} in the xylyl species [**3a-h**]CF_3SO_3 and at ca. 1690 cm^{-1} in complexes [**4a-d**]CF_3SO_3, containing two N-bound methyl substituents. The C^1-N bond possesses a double bond character, therefore the two methyl groups resonate at distinct chemical shifts in the NMR spectra of [**4a-d**]CF_3SO_3 [e.g. in the case of [**4a**]CF_3SO_3, acetone-d_6 solution: $\delta(^1H)$ = 4.06, 3.48 ppm; $\delta(^1H)$ = 51.3, 44.4 ppm]. Consistently, the ^1H NMR spectra of [**3a-h**]CF_3SO_3 exhibit two sets of resonances attributed to E and Z isomers, with the E form largely prevailing. The ^{13}C NMR spectra contain the diagnostic resonance related to C^1 within a typical region for an amino-alkylidene (224 – 233 ppm); the vinyl C^2 carbon resonates at ca. 54 ppm, instead the C^3 resonance is found at low fields (198 – 208 ppm) as a result of a significant bridging-alkylidene character. ^{19}F NMR analysis was performed on those compounds containing a F-substituted ring, and for instance the ^1H-decoupled ^{19}F NMR spectrum of [**5b**]CF_3SO_3 contains two resonances at −113.1 ppm (aryl fluoride) and −78.6 ppm (triflate anion). The reactions of [**3a-h**]CF_3SO_3 and [**4a-d**]CF_3SO_3 with an excess of pyrrolidine were carried out in tetrahydrofuran, and afforded the mononuclear derivatives **5a-h** and **6a-c**; after work-up, these products were isolated in 55-84% yields, apart from **6b** (30%). This series of compounds, excluded **5h** and **6c**, is unprecedented. The characterization was performed by means of IR and NMR spectroscopy, moreover the molecular structures of **5a, 5h** and **6b** were ascertained by X-ray diffraction studies (Figure 1, Table 1). Such X-ray structures share a 1-metalla-2-aminocyclopenta-1,3-dien-5-one five-membered ring core.[18,20,21] The C^2-C^3 bond is essentially a double one [1.319(8) Å in **5a**, 1.348(8) Å in **5a**, 1.327(7) Å in **5a**], while C^1-N holds some double bond character [e.g. 1.320(7) Å in the case of **6b**], with **5a** and **5h** exhibiting the E configuration for the

N-substituents. The OH group in **5h** is involved in an intermolecular hydrogen bond with the C(4)O(2) group of an adjacent molecule [O(3)-H(3) 0.82 Å, H(3)···O(2)#1 1.93 Å, O(3)···O(2)#1 2.733(7) Å, <O(3)H(3)O(2)#1 167.2°, #1 -x+1, -y, -z+1]. Also the NH_2 group of **6b** forms an interesting H-bond, involving the O(2) atom of the same molecule [N(2)-H(22) 0.87(2) Å, H(22)···O(2) 2.31(5) Å, N(2)···O(2) 3.040(7) Å, <N(2)H(22)O(2) 142(7)°], the O(2) atom of an adjacent molecule [N(2)-H(21) 0.86(2) Å, H(21)···O(2)#1 2.49(4) Å, N(2)···O(2)#1 3.250(7) Å, <N(2)H(21)O(2)#1 148(6)°, #1 -x+1/2, y+1/2, z], and the chloride of a CH_2Cl_2 molecule [N(2)-H(22) 0.87(2) Å, H(22)···Cl(1) 2.88(5) Å, N(2)···Cl(1) 3.613(7) Å, <N(2)H(22)Cl(1) 143(6)°].

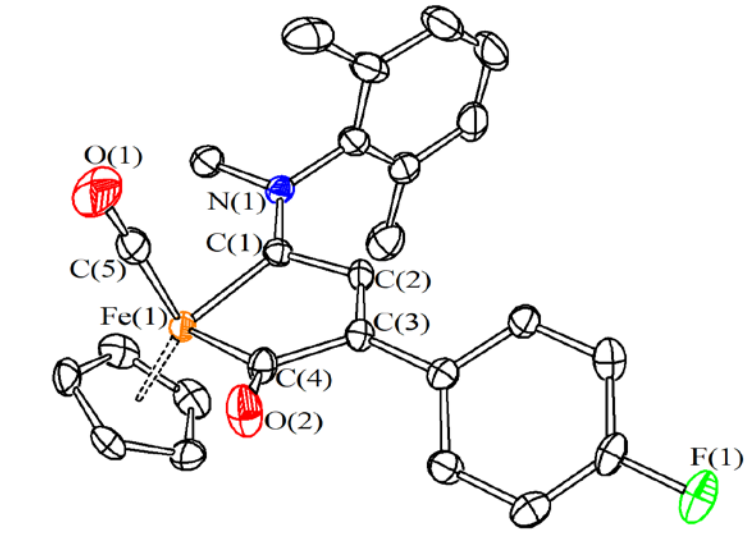

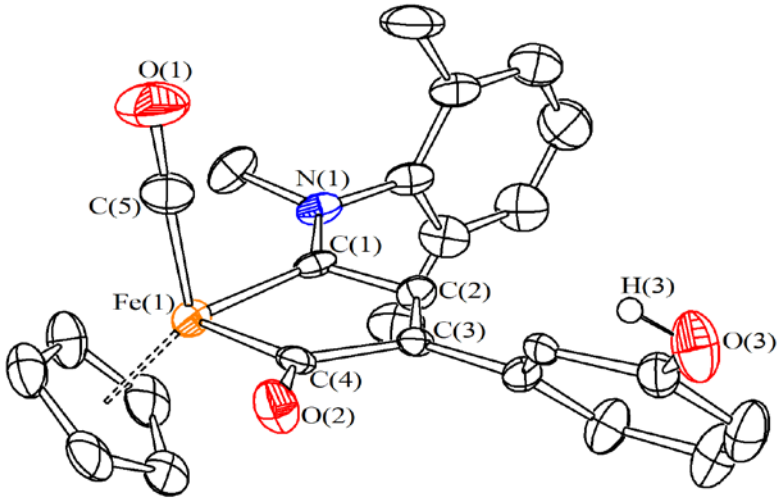

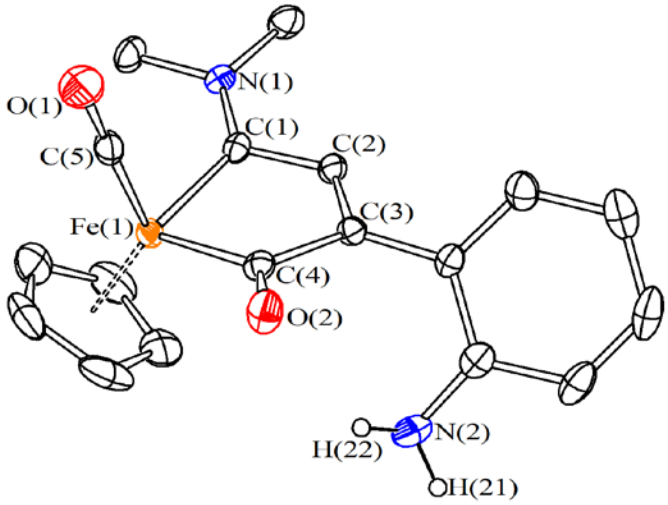

Figure 1. Molecular structures of (a) [FeCp(CO){C^1NMe(Xyl)C^2HC^3(4-C_6H_4F)C(=O)}], **5a**, (b) [FeCp(CO){C^1NMe(Xyl)C^2HC^3(3-C_6H_4OH)C(=O)}], **5h**, and (c) [FeCp(CO){C^1N$(Me)_2$$C^2HC^3$(2-$C_6H_4NH_2$)C(=O)}], **6b**. Displacement ellipsoids are at the 30% probability level. H-atoms, except those bonded to O and N-atoms, have been omitted for clarity.

Table 1. Selected bond distances (Å) and angles (°) for **5a**, **5h** and **6b**.

	5a	**5h**	**6b**
Fe(1)-C(5)	1.738(6)	1.725(8)	1.732(6)
Fe(1)-C(4)	1.948(5)	1.927(6)	1.926(6)
Fe(1)-C(1)	1.913(5)	1.916(7)	1.932(6)
C(5)-O(1)	1.144(8)	1.151(8)	1.129(7)
C(4)-O(2)	1.197(7)	1.225(7)	1.224(6)
C(3)-C(4)	1.530(7)	1.506(9)	1.531(7)
C(2)-C(3)	1.319(8)	1.348(8)	1.327(7)
C(1)-C(2)	1.460(7)	1.457(9)	1.452(7)
C(1)-N(1)	1.311(7)	1.314(8)	1.320(7)
C(1)-Fe(1)-C(4)	83.3(2)	83.4(3)	82.4(2)
Fe(1)-C(4)-C(3)	111.3(4)	113.3(5)	112.4(4)
C(4)-C(3)-C(2)	112.3(5)	112.7(6)	111.4(5)
C(3)-C(2)-C(1)	117.0(5)	115.4(6)	116.6(5)
C(2)-C(1)-Fe(1)	113.1(4)	114.1(5)	113.1(4)
Fe(1)-C(5)-O(1)	178.0(7)	178.5(9)	178.8(6)

The IR spectra of **5a-h** and **6a-b** (in CH_2Cl_2) are featured by an intense band due to the single carbonyl ligand around 1920 cm^{-1}, and additional weak bands related to the acyl (1601 - 1664 cm^{-1}) and C^1-N (1579 - 1605

cm^{-1}) bonds. In general, the NMR spectra of **5a-h** contain a single set of resonances, attributed to the E isomer with reference to the N-substituents, in analogy with what detected for the parent vinyliminium compounds and for **5a** and **5h** in the solid state (see above X-ray diffraction studies), the only exception being **5g** (E and Z isomers in 5:1 relative ratio). In the NMR spectra of **6a-c**, the two methyl groups are non equivalent, in agreement with the partial double bond nature of C^1-N; for instance, they resonate at 51.8 and 44.0 ppm in the ^{13}C spectrum of **6c**. The amino-alkylidene character of C^1 is reflected by a typical low-field resonance (256.4 – 265.6 ppm). Instead, the resonance for the C^2-hydrogen falls in within a region (6.80 – 8.03 ppm) indicative of the alkenic character.

It should be remarked that the structural motif contained in **5a-h** and **6a-b** comprises a unusual aminoalkylidene moiety, which is pre-formed in the diiron precursor and is maintained in the monoiron derivative, the conversion reaction being tolerant of various functional groups (e.g. alcohol, amine). On the other hand, the introduction of an amino-alkylidene group in half-sandwich iron complexes by classical methods requires the modification of a hydrocarbyl ligand, e.g. via aminolysis of an alkoxy-alkylidene [26] or a vinylidene,[27] or derivatization of an isocyanide.[26a]

In view of the biological trials, [**3a**]CF_3SO_3, **5a**, **5e**, **5g** and **5h** were selected as model compounds for a stability study in aqueous media. Thus, a substantial fraction (60-80%) of each iron compound was detected after being stored at 37 °C for 48 hours in dmso-d_6/D_2O solution, as determined by ^1H NMR spectroscopy (Table S1). More detailed analyses were carried out using a mixture of dmso-d_6 and deuterated cell culture medium as solvent (see Experimental); interestingly, ^1H NMR experiments revealed a considerable stability of the compounds under these conditions, with 75-80% of the starting amount being recognized after 24 hours at 37 °C (Table 5). The slow degradation process is paralleled by the formation of a brown precipitate, presumably iron oxide(s),[18] and the evolution of carbon monoxide, checked by gas chromatography. More precisely, 0.4-0.5 equivalents of CO were determined to be released from each compound; a comparison with the stability data (Table 5) indicates that the degradation of the piano-stool derivatives takes place with dissociation of the CO ligand and also rupture of the metallacycle, eliminating the acyl moiety as a second CO molecule.

3. Biological Activity and catalytic NADH oxidation

The antiproliferative activity of compounds [**3d**]CF_3SO_3, [**4a-d**]CF_3SO_3, **5a-h** and **6a-b** was assessed against cisplatin sensitive and cisplatin resistant human ovarian carcinoma (A2780 and A2780cisR) cell lines and the non-tumorigenic human embryonic kidney (HEK-293) cell line. Cisplatin was evaluated as a positive control. The obtained IC_{50} values are compiled in Table 2, together with those previously determined for **6c**.[23] Among the diiron ionic species, [**3d**]CF_3SO_3 exhibits the highest cytotoxicity against the A2780 and A2780cisR cell lines, being the IC_{50} values respectively similar and ca. 20-fold times lower than the corresponding ones of cisplatin. The monoiron complexes **5a-h** are featured by a comparable, moderate cytotoxic activity against the three

investigated cell lines, while **6a-b** are significantly less cytotoxic**.** In general, the presence of the xylyl substituent (instead of a methyl) on the aminoalkylidene function imparts a superior activity, in both mono and diiron types of complexes (compare the data related to [**3d**]CF_3SO_3 and [**3d**]CF_3SO_3**,** and of **5b** and **6b**, respectively). Conversely, the nature and the position of the substituent(s) on the C^3-bound aryl group do not seem to significantly affect the IC_{50} values.

Table 2. IC_{50} values (μM) determined for iron compounds and cisplatin on human ovarian carcinoma (A2780), human ovarian carcinoma cisplatin resistant (A2780CisR) and human embryonic kidney (HEK-293) cell lines after 72 h exposure. Values are given as the mean ± SD.

Compnd.	Compnd.	A2780	A2780cisR	HEK-293
MeXy 4Me	[**3d**]CF_3SO_3	1.1 ± 0.4	0.9 ± 0.2	0.75 ± 0.06
MeMe 4F	[**4a**]CF_3SO_3	17.4 ± 0.8	20 ± 2	35 ± 3
MeMe NH2	[**4b**]CF_3SO_3	25 ± 3	34 ± 4	33 ± 3
MeMe 2CF3	[**4c**]CF_3SO_3	20 ± 3	25 ± 4	30 ± 2
MeMe 4Me	[**4d**]CF_3SO_3	8 ± 2	17.0 ± 1.0	18 ± 2
MeXy 4F	**5a**	7.6 ± 1.5	7.4 ± 0.9	5.6 ± 1.1
MeXyl 3F	**5b**	10 ± 2	10.2 ± 0.3	14.4 ± 1.4
MeXy 2F	**5c**	11 ± 2	11.5 ± 1.1	9.7 ± 0.9
MeXy 4Me	**5d**	10 ± 2	8.9 ± 1.0	8.1 ± 0.8
MeXy 3Me	**5e**	10 ± 2	17 ± 3	7.4 ± 1.2
MeXy Bifenile	**5f**	12 ± 2	14.8 ± 1.5	11 ± 2
MeXy NH2	**5g**	16 ± 2	10.5 ± 1.0	27 ± 2
MeXy OH	**5h**	14 ± 2	10 ± 3	11.2 ± 0.6
MeMe 4F	**6a**	22 ± 2	20 ± 5	35 ± 3
MeMe NH2	**6b**	56 ± 4	33 ± 2	43 ± 3
MeMe 2CF3 [23]	**6c**	37 ± 3	22 ± 3	44 ± 10
cisplatin	cisplatin	1.5 ± 0.5	18.9 ± 0.7	2.4 ± 0.7

Previous studies indicated that the in vitro antiproliferative activity of diiron and monoiron vinyl-aminoalkylidene complexes, analogous to those reported here, is mainly attributable to redox processes involving the Fe(II) centres. More precisely, both the reduction/oxidation of cationic/neutral complexes in a physiological environment and the progressive, slow degradation of the complexes are probably contributing. As a matter of fact, a series of such diiron and monoiron compounds revealed to trigger a significant ROS production.[18,23] In order to further investigate this point, we selected some of the complexes here reported for a study on their ability to catalyze the aerobic oxidation of NADH, by means of an established UV-Vis spectroscopic method (see Experimental and Table 3).[28] It should be remarked that nicotinamide adenine dinucleotide (NAD^+) and its reduced form (NADH) are crucial cofactors for the maintenance of redox balance in cells,[29] and the

modification of the NADH/NAD^+ ratio has been associated to the anticancer activity of various late transition metal complexes.[28,30] Among the monoiron complexes, **5a** exhibited a clear efficacy to promote NADH oxidation, being its catalytic activity significantly enhanced respect to that of the parent compound [**3a**]CF_3SO_3 (Table 3). However, the TON values provided by **5e** and **5h** were slightly higher compared to the reference and, surprisingly, **5g** was able to slightly retard the oxidation of NADH with respect to the blank experiment.

Table 3. Turnover numbers (TON) of iron compounds (10 μM) in the aerobic oxidation of NADH (220 μM) in a 5% DMSO phosphate buffered solution at 37 °C after 25 hours. $FeSO_4$ used as a reference compound.

Compound	TON
[3a]CF_3SO_3	2.9
5a	3.8
5e	2.5
5g	1.9
5h	2.5
$FeSO_4$ [a]	2.2

[a]NADH oxidation over time not significantly different from the blank experiment.

The iron compounds were also assessed for their antibacterial activity against pathogens endowed with a high rate of antibiotic resistance. The minimum inhibitory concentrations (MIC), that is, the lowest concentration of the tested drugs able to inhibit the bacterial growth, were determined, and the results are compiled in Table 4. The majority of the complexes evidenced absence of activity. However, three cationic diiron complexes, i.e. **[3d,i]**CF_3SO_3 and **[4d]**CF_3SO_3, exhibited some activity against Gram positive bacteria, the lack of activity towards Gram negative strains being presumably due to the additional outer membrane resulting in a low permeability barrier. Remarkably, the most potent complex in terms of antibacterial activity, i.e. [**3d]**CF_3SO_3, is also the most effective cytotoxic agent. In general, the trend of pronounced biological effect of those complexes containing the xylyl group, compared to the homologous ones with a methyl substituent, seems confirmed in the data reported in Table 4.

Table 4. Minimal inhibitory concentrations (MIC, μM) of the iron compounds and cisplatin against pathogenic strains endowed with antibiotic resistance.

Compnd.	Compnd.	*P. aeruginosa*	*A.baumanii*	*S. aureus*	*E. faecium*
MeXy 4Me	[**3d**]CF_3SO_3	100	>100	6.2	12.5
MeXy tBu	[**3i**]CF_3SO_3	100	100	12.5	75
MeMe 4F	[**4a**]CF_3SO_3	>100	>100	>100	>100
MeMe NH2	[**4b**]CF_3SO_3	>100	>100	>100	>100

MeMe 2CF3	[**4c**]CF_3SO_3	>100	>100	100	100
MeMe 4Me	[**4d**]CF_3SO_3	>100	>100	50	100
MeXy 4F	**5a**	>100	>100	>100	>100
MeXy 3F	**5b**	>100	>100	>100	>100
MeXy 2F	**5c**	>100	>100	>100	>100
MeXy 4Me	**5d**	>100	>100	>100	>100
MeXy 3Me	**5e**	>100	>100	>100	>100
MeXy Bifenile	**5f**	>100	>100	>100	100
MeXy NH2	**5g**	>100	>100	>100	100
MeXy OH	**5h**	>100	>100	>100	>100
MeMe 4F	**6a**	>100	>100	>100	100
MeMe NH2	**6b**	>100	>100	>100	>100
~~cisplatin~~	~~cisplatin~~	~~>100~~	~~>100~~	~~>100~~	~~>100~~

Conclusions

Despite the interest of medicinal chemistry in the development of both ferrocene derivatives and iron carbonyl compounds in view of different applications, biological studies on iron complexes containing at the same time cyclopentadienyl and carbonyl ligands are rather sparse in the literature. Herein, we have described the synthesis of a number of new di- and monoiron cyclopentadienyl carbonyl complexes, all featured by an additional vinyl-aminoalkylidene moiety. The two categories of compounds are related to each other, in that monoiron complexes are prepared from the diiron precursors, where the C_3 hydrocarbyl chain is assembled, according to a general reaction. The compounds have been assessed for their in vitro antiproliferative activity towards cancer and non cancer cell lines, and also for their antimicrobial activity against clinically relevant pathogens with a high rate of antibiotic resistance. In general, the compounds are rather stable in aqueous media and cytotoxic, with IC_{50} values in the low micromolar/nanomolar range, although lacking of selectivity. Interestingly, some of the complexes are able to sensitize cisplatin resistant A2780cisR cells at relatively low concentrations. Experiments confirm the interference with cellular redox mechanisms as a viable mode of action, in accordance with previous studies; the slow but progressive degradation of the complexes in the biological environment may play a key role, resulting in the release of Fe^{2+} cations[31] and carbon monoxide. The most cytotoxic complex of the series, i.e. [**3d**]CF_3SO_3, displays also an appreciable ability to inhibit Gram positive bacterial growth.

Experimental

1) Materials and methods. All the operations were carried out under N_2 atmosphere using standard Schlenk techniques. The reaction vessels were oven dried at 140°C prior to use, evacuated (10^{-2} mmHg) and then filled with N_2. Organic reactants (TCI Europe or Merck) were commercial products of the highest purity available. Compounds $[Fe_2Cp_2(CO)_2(\mu\text{-}CO)\{\mu\text{-}CNMe(R)\}]CF_3SO_3$ (R = Xyl = 2,6-$C_6H_3Me_2$, [**1**]CF_3SO_3; R = Me, [**2**]CF_3SO_3),[25] $[Fe_2Cp_2(CO)(\mu\text{-}CO)\{\mu\text{-}\eta^1\text{:}\eta^3\text{-}C(3\text{-}C_6H_4OH)CHCN(Me)(Xyl)\}]CF_3SO_3$, [**3h**]$CF_3SO_3$,[18] $[Fe_2Cp_2(CO)(\mu\text{-}CO)\{\mu\text{-}\eta^1\text{:}\eta^3\text{-}C(^tBu)CHCN(Me)(Xyl)\}]CF_3SO_3$, [**3i**]$CF_3SO_3$,[23] and $[Fe_2Cp_2(CO)(\mu\text{-}CO)\{\mu\text{-}\eta^1\text{:}\eta^3\text{-}C(3,5\text{-}C_6H_3(CF_3)_2)CHCN(Me)(Xyl)\}]CF_3SO_3$,[23] [**4d**]$CF_3SO_3$, were prepared according to published procedures. Solvents were distilled before use under N_2 from appropriate drying agents. Chromatography separations were carried out under N_2 on columns of deactivated alumina (Sigma Aldrich, 4% *w/w* water). Infrared spectra of solid samples were recorded on a Perkin Elmer Spectrum One FT-IR spectrometer, equipped with a UATR sampling accessory (4000-400 cm^{-1} range). Infrared spectra of solutions were recorded on a Perkin Elmer Spectrum 100 FT-IR spectrometer with a CaF_2 liquid transmission cell (2300-1500 cm^{-1} range). IR spectra were processed with Spectragryph software.[32] UV-Vis spectra (190-900 nm) were recorded on a Ultraspec 2100 Pro spectrophotometer with 1.0 cm PMMA cuvettes. NMR spectra were recorded at 298 K on a Bruker Avance II DRX400 instrument equipped with a BBFO broadband probe. Chemical shifts (expressed in parts per million) are referenced to the residual solvent peaks [33] (^1H, ^{13}C) or to external standard (^{19}F, $CFCl_3$). NMR spectra were assigned with the assistance of ^1H-^{13}C (*gs*-HSQC and *gs*-HMBC) correlation experiments.[34] NMR signals due to a second isomeric form (where it has been possible to clearly detect them) are italicized. Carbon, hydrogen and nitrogen analyses were performed on a Vario MICRO cube instrument (Elementar). GC analysis was performed on a Clarus 500 instrument (PerkinElmer) equipped with a 5Å MS packed column (Supelco) and a TCD detector. Samples were analyzed by isothermal runs (110 °C, 3 min) using He as carrier gas.

2) Synthesis and characterization of diiron compounds. *General procedure:* $[Fe_2Cp_2(CO)_2(\mu\text{-}CO)\{\mu\text{-}CNMe(R)\}]CF_3SO_3$ (ca. 0.5 mmol; R = Xyl = 2,6-$C_6H_3Me_2$, [**1**]CF_3SO_3; R = Me, [**2**]CF_3SO_3) was dissolved into acetonitrile (10 mL), then Me_3NO (1.3 eq.) was added. The resulting mixture was stirred for 1 hour, during which progressive colour darkening was observed. The complete conversion of the starting material into $[Fe_2Cp_2(CO)(\mu\text{-}CO)(NCMe)\{\mu\text{-}CNMe(R)\}]CF_3SO_3$ was checked by IR spectroscopy. The volatiles were removed under vacuum, thus the dark brown residue was dissolved into dichloromethane (ca. 20 mL). The solution was treated with the appropriate alkyne (ca. 1.3 eq.), and the mixture was stirred at room temperature for 48 hours. The final mixture was charged on an alumina column. Elution with CH_2Cl_2 and CH_2Cl_2/THF mixtures allowed to remove unreacted alkyne

and impurities, then a fraction corresponding to the desired product was collected using neat MeOH as eluent. Removal of the solvent under reduced pressure afforded air stable products.

$[Fe_2Cp_2(CO)(\mu\text{-}CO)\{\mu\text{-}\eta^1\text{:}\eta^3\text{-}C^3(4\text{-}C_6H_4F)C^2HC^1N(Me)(Xyl)\}]CF_3SO_3$, [3a]$CF_3SO_3$ (Chart 1).

Chart 1. Structure of [**3a**]$^+$.

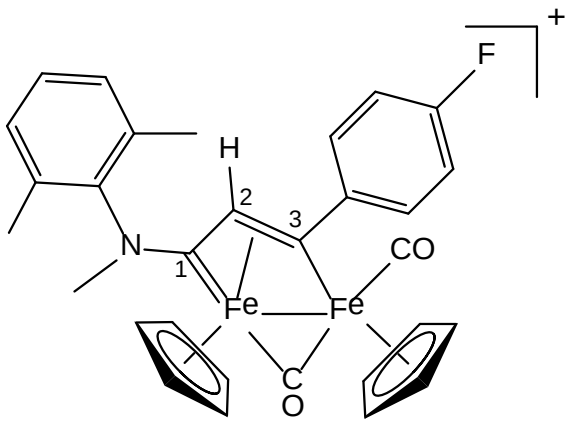

From [**1**]CF_3SO_3 and 1-ethynyl-4-fluorobenzene.[35] Brown solid, yield 66%. Anal. calcd. for $C_{31}H_{27}F_4Fe_2NO_5S$: C, 52.20; H, 3.82; N, 1.96. Found: C, 52.10; H, 3.74; N, 2.02. IR (CH_2Cl_2): ũ/cm^{-1} = 2003vs (CO), 1818s (μ-CO), 1630m (C^2C^1N), 1601w (arom C-C). ^{1}H NMR (acetone-d_6): δ/ppm = 7.64, 7.28-7.18, 7.09 (m, 7 H, C_6H_4F + $C_6H_3Me_2$); 5.68, 5.42, *5.37*, *5.07* (s, 10 H, Cp); 4.42, *3.75* (s, 3 H, NMe); 4.31 (s, 1 H C^2H); *2.51*, 2.35, *2.09*, 1.89 (s, 6 H, $C_6H_3Me_2$). E/Z ratio = ca. 15. $^{13}C\{^1H\}$ NMR (acetone-d_6): δ/ppm = 253.4 (μ-CO); 232.3 (C^1); 210.3 (CO); 206.3 (C^3); 161.6 (d, $^1J_{CF}$ = 245 Hz, CF); 152.3, 128.9 (d, $^3J_{CF}$ = 7.5 Hz), 115.3 (d, $^2J_{CF}$ = 20.7 Hz) (C_6H_4F); 145.5 (*ipso*-$C_6H_3Me_2$); 132.0, 131.3, 129.6, 129.3 ($C_6H_3Me_2$); 121.6 (q, $^1J_{CF}$ = 322 Hz, CF_3); 92.5, *92.3*, 88.2, *87.9* (Cp); 54.0 (C^2); 45.5 (NMe); 17.3, 16.6 ($C_6H_3Me_2$). $^{19}F\{^1H\}$ NMR (acetone-d_6): δ/ppm = −78.7 (CF_3SO_3); −117.3 (C_6H_4F).

$[Fe_2Cp_2(CO)(\mu\text{-}CO)\{\mu\text{-}\eta^1\text{:}\eta^3\text{-}C^3(3\text{-}C_6H_4F)C^2HC^1N(Me)(Xyl)\}]CF_3SO_3$, [3b]$CF_3SO_3$ (Chart 2).

Chart 2. Structure of [**3b**]$^+$.

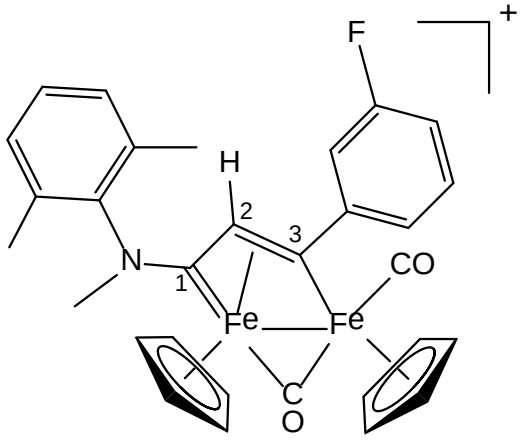

From [**1**]CF_3SO_3 and 1-ethynyl-3-fluorobenzene. Brown solid, yield 80%. Anal. calcd. for $C_{31}H_{27}F_4Fe_2NO_5S$: C, 52.20; H, 3.82; N, 1.96. Found: C, 52.41; H, 3.78; N, 1.90. IR (CH_2Cl_2): ũ/cm^{-1} = 2005vs (CO), 1820s (μ-CO), 1629m (C^2C^1N), 1606w (arom C-C). ^{1}H NMR (dmso-d_6): δ/ppm = 7.64, 7.28-7.18, 7.09 (m, 7 H, C_6H_4F + $C_6H_3Me_2$); 5.73, 5.45, *5.39*, *5.12* (s, 10 H, Cp); 4.45 (s, 1 H C^2H); 4.44, *3.78* (s, 3 H, NMe); 2.35, 1.89 (s, 6 H, $C_6H_3Me_2$). E/Z ratio = ca. 10. $^{13}C\{^1H\}$ NMR (CD_2Cl_2): δ/ppm = 252.3 (*μ*-CO); 231.5 (C^1); 209.3 (CO); 204.9 (C^3); 157.5, 131.3, 130.6, 129.7, 129.3, 122.8, 114.0, 113.2 ($C_6H_3Me_2$ + C_6H_4F); 145.1 (*ipso*-$C_6H_3Me_2$); 92.3, 87.9, *88.6* (Cp); 46.0 (NMe); 17.9, 17.1 ($C_6H_3Me_2$). C^2 overlapped with solvent signal. $^{19}F\{^1H\}$ NMR (CD_2Cl_2): δ/ppm = −78.6 (CF_3SO_3); −113.1 (C_6H_4F).

[Fe_2Cp_2(CO)(μ-CO){μ-η^1:η^3-C^3(2-C_6H_4F)C^2HC^1N(Me)(Xyl)}]CF_3SO_3, [3c]CF_3SO_3 (Chart 3).

Chart 3. Structure of [**3c**]$^+$.

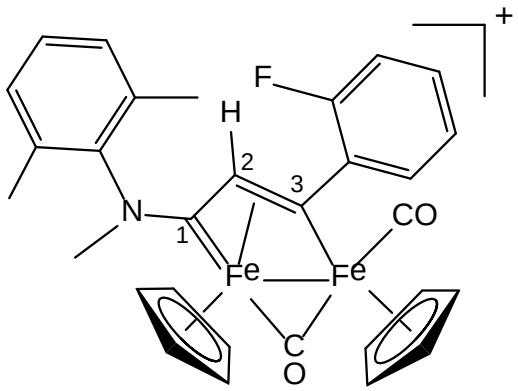

From [**1**]CF_3SO_3 and 1-ethynyl-2-fluorobenzene. Brown solid, yield 94%. Anal. calcd. for $C_{31}H_{27}F_4Fe_2NO_5S$: C, 52.20; H, 3.82; N, 1.96. Found: C, 51.95; H, 3.77; N, 2.00. IR (CH_2Cl_2): ũ/cm^{-1} = 2010vs (CO), 1820s (μ-CO), 1630m (C^2C^1N), 1587w (arom C-C). ^{1}H NMR (acetone-d_6): δ/ppm = 7.82-7.03 (m, 7 H, C_6H_4F + $C_6H_3Me_2$); 5.42, 5.18, *5.12*, *4.96* (s, 10 H, Cp); 4.28, *3.58* (s, 3 H, NMe); 4.09 (s, 1 H C^2H); *2.53*, 2.23, *2.07*, 1.85 (s, 6 H, $C_6H_3Me_2$). E/Z ratio = ca. 5. $^{13}C\{^1H\}$ NMR (acetone-d_6): δ/ppm = 252.2 (*μ*-CO); 231.5 (C^1); 208.9 (CO); 198.2 (C^3); 156.5 (d, $^1J_{CF}$ = 247 Hz, CF); 145.2 (*ipso*-$C_6H_3Me_2$); 142.5, 131.2, 129.9-129.1, 124.8, 115.7 (C_6H_4F + $C_6H_3Me_2$); 121.0 (q, $^1J_{CF}$ = 322 Hz, CF_3); 92.0, 87.6 (Cp); 55.1 (C^2); 45.8 (NMe); 17.8, *17.7*, 17.1 ($C_6H_3Me_2$). $^{19}F\{^1H\}$ NMR (acetone-d_6): δ/ppm = −78.6 (CF_3SO_3); −112.5 (C_6H_4F).

[Fe_2Cp_2(CO)(μ-CO){μ-η^1:η^3-C^3(4-C_6H_4Me)C^2HC^1N(Me)(Xyl)}]CF_3SO_3, [3d]CF_3SO_3 (Chart 4).[19a]

Chart 4. Structure of [**3d**]$^+$.

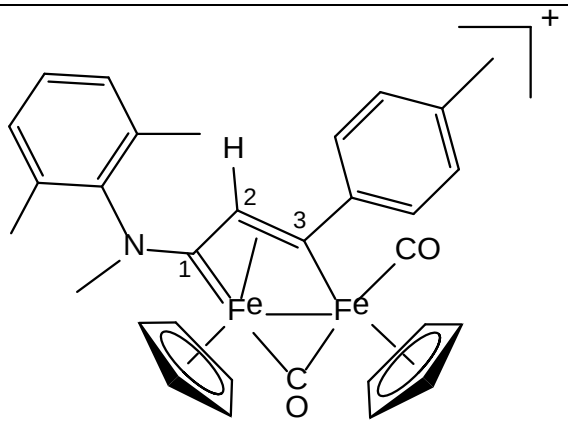

From [**1**]CF_3SO_3 and 4-ethynyltoluene. Brown solid, yield 72%. Anal. calcd. for $C_{32}H_{30}F_3Fe_2NO_5S$: C, 54.18; H, 4.26; N, 1.97. Found: C, 54.03; H, 4.36; N, 2.05. IR (CH_2Cl_2): ũ/cm^{-1} = 2002vs (CO), 1817s (μ-CO), 1630m (C^2C^1N). ^{1}H NMR ($CDCl_3$): δ/ppm = 7.34 (d, *J* = 7.9 Hz, 2H, C_6H_4Me), 7.29 (d, *J* = 8.2 Hz, 2H, C_6H_4Me), 7.18 (t, *J* = 7.6 Hz, 1H, $C_6H_3Me_2$), 7.07 (d, *J* = 7.7 Hz, 1H, $C_6H_3Me_2$), 6.98 (d, *J* = 7.5 Hz, 1H, $C_6H_3Me_2$); 5.38, 5.17, *5.09*, *4.89* (s, 10H, Cp); *4.77*, 3.94 (s, 1H, C^2H); 4.25, *3.59* (s, 3H, NMe); *2.53*, 2.21, *2.01*, 1.81 (s, 6H, $C_6H_3Me_2$); *2.47*, 2.42 (s, 3H, C_6H_4Me). E/Z ratio = 10:1. $^{13}C\{^1H\}$ NMR ($CDCl_3$): δ/ppm = 253.5, *253.4* (μ-CO); 232.1, *230.6* (C^1); *210.4*, 209.7 (CO); 208.1, *207.6* (C^3); *153.2*, 153.1 (*ipso*-C_6H_4Me); *153.2*, 145.1, *140.8* (*ipso*-C_6H_3); 137.6-126.4 ($C_6H_3Me_2$ + C_6H_4Me); 92.2, *92.1*, 88.0, *87.8* (Cp); 53.5, *53.4* (C^2); *52.4*, 45.9 (NMe); *21.2*, 21.1 (C_6H_4Me); *17.9*, 17.8, 17.2 ($C_6H_3Me_2$).

[Fe_2Cp_2(CO)(μ-CO){μ-η^1:η^3-C^3(3-C_6H_4Me)C^2HC^1N(Me)(Xyl)}]CF_3SO_3, [3e]CF_3SO_3 (Chart 5).

Chart 5. Structure of [**3e**]$^+$.

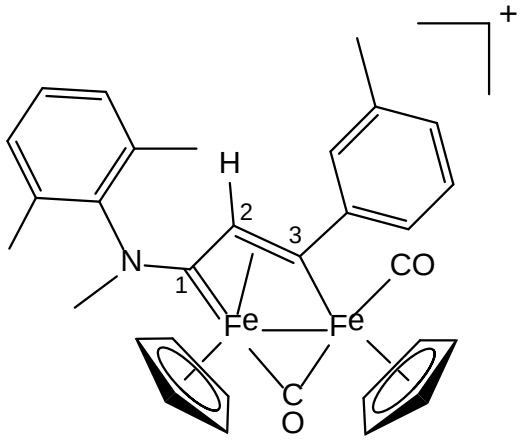

From [**1**]CF_3SO_3 and 3-ethynyltoluene. Brown solid, yield 82%. Anal. calcd. for $C_{32}H_{30}F_3Fe_2NO_5S$: C, 54.18; H, 4.26; N, 1.97. Found: C, 54.31; H, 4,33; N, 1.93. IR (CH_2Cl_2): ũ/cm^{-1} = 2003vs (CO), 1817s (μ-CO), 1631m (C^2C^1N). ^{1}H NMR (acetone-d_6): δ/ppm = 7.72-7.09 (m, 7 H, $C_6H_3Me_2$ + C_6H_4Me); 5.67, 5.38 (s, 10 H, Cp); 4.41 (s, 3 H, NMe); 4.23 (s, 1 H, C^2H); 2.42 (s, 3 H, C_6H_4Me); 2.34, 1.88 (s, 6 H, $C_6H_3Me_2$). $^{13}C\{^1H\}$ NMR (acetone-d_6): δ/ppm =

253.9 (μ-CO); 232.3 (C^1); 210.5 (CO); 208.3 (C^3); 156.1 (*ipso*-C_6H_4Me); 145.5 (*ipso*-$C_6H_3Me_2$); 137.9, 132.1, 131.3, 129.6, 129.4, 128.4, 127.7, 126.9, 124.1 (C_6H_4Me + $C_6H_3Me_2$); 92.5, 88.3 (Cp); 53.5 (C^2); 46.7 (NMe); 20.8 (C_6H_4Me); 17.5, 16.7 ($C_6H_3Me_2$).

$[Fe_2Cp_2(CO)(\mu\text{-}CO)\{\mu\text{-}\eta^1\text{:}\eta^3\text{-}C^3(4\text{-}C_6H_4Ph)C^2HC^1N(Me)(Xyl)\}]CF_3SO_3$, $[\mathbf{3f}]CF_3SO_3$ (Chart 6).

Chart 6. Structure of $[\mathbf{3f}]^+$.

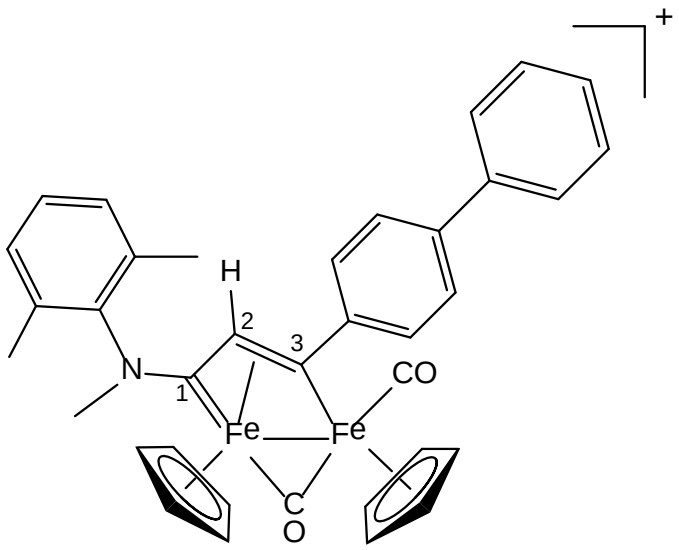

From [**1**]CF_3SO_3 and 4-ethynylbiphenyl. Brown solid, yield 78%. Anal. calcd. for $C_{37}H_{32}F_3Fe_2NO_5S$: C, 57.61; H, 4.18; N, 1.82. Found: C, 57.43; H, 4.24; N, 1.69. IR (CH_2Cl_2): $\tilde{\upsilon}/cm^{-1}$ = 2003vs (CO), 1818s (μ-CO), 1628m (C^2C^1N). ^1H NMR (acetone-d_6): δ/ppm = 8.05-7.10 (m, 12 H, $C_{12}H_9$ + $C_6H_3Me_2$); 5.70, 5.45, *5.40*, *5.10* (s, 10 H, Cp); 4.45, *3.78* (s, 3 H, NMe); *4.72*, 4.36 (s, 1 H C^2H); *2.63*, 2.37, *2.11*, 1.91 (s, 6 H, $C_6H_3Me_2$). E/Z ratio = 5. $^{13}C\{^1H\}$ NMR (acetone-d_6): δ/ppm = 253.6 (μ-CO); 232.4 (C^1); 210.4 (CO); 207.2 (C^3); 153.3 (*ipso*-C_6H_4); 145.5 (*ipso*-$C_6H_3Me_2$); 140.1, 139.5, 134.1, 132.0, 131.3, 129.6, 129.3, 129.0, 128.4, 127.6, 127.5, 126.8, 126.7, 126.6 ($C_6H_3Me_2$ + $C_{12}H_9$); 92.5, *92.4*, 88.1, *87.9* (Cp); 53.4 (C^2); 45.5 (NMe); 17.3, 16.6 ($C_6H_3Me_2$).

$[Fe_2Cp_2(CO)(\mu\text{-}CO)\{\mu\text{-}\eta^1\text{:}\eta^3\text{-}C^3(2\text{-}C_6H_4NH_2)C^2HC^1N(Me)(Xyl)\}]CF_3SO_3$, $[\mathbf{3g}]CF_3SO_3$ (Chart 7).

Chart 7. Structure of $[\mathbf{3g}]^+$.

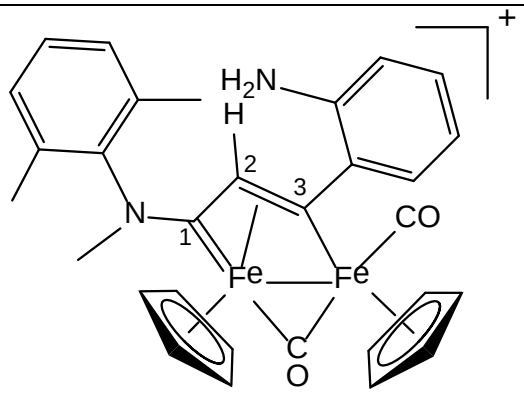

From [**1**]CF_3SO_3 and 2-ethynylaniline. Brown solid, yield 81%. Anal. calcd. for $C_{31}H_{29}F_3Fe_2N_2O_5S$: C, 52.42; H, 4.12; N, 3.94. Found: C, 52.26; H, 4.18; N, 4.02. IR (CH_2Cl_2): ũ/cm^{-1} = 1992vs (CO), 1819s (μ-CO), 1626s (C^2C^1N). ^{1}H NMR (acetone-d_6): δ/ppm = 8.05-7.10 (m, 12 H, $C_{12}H_9$ + $C_6H_3Me_2$); 5.71, 5.37, *5.31*, *5.11* (s, 10 H, Cp); 4.45, *3.73* (s, 3 H, NMe); 4.31 (s, 1 H C^2H); 2.34, 1.90 (s, 6 H, $C_6H_3Me_2$).

[$Fe_2Cp_2(CO)(\mu\text{-}CO)\{\mu\text{-}\eta^1\text{:}\eta^3\text{-}C^3(4\text{-}C_6H_4F)C^2HC^1NMe_2\}$]$CF_3SO_3$, [4a]$CF_3SO_3$ (Chart 8).

Chart 8. Structure of [**4a**]$^+$.

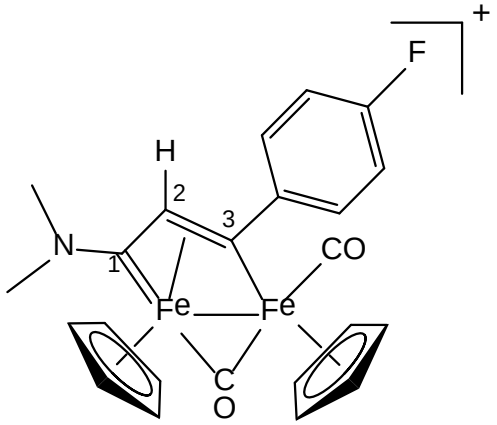

From [**2**]CF_3SO_3 and 1-ethynyl-4-fluorobenzene. Brown solid, yield 68%. Anal. calcd. for $C_{24}H_{21}F_4Fe_2NO_5S$: C, 46.26; H, 3.40; N, 2.25. Found: C, 46.46; H, 3.29; N, 2.26. IR (CH_2Cl_2): ũ/cm^{-1} = 1992vs (CO), 1808s (μ-CO), 1690m (C^2C^1N). ^{1}H NMR (acetone-d_6): δ/ppm = 7.92, 7.31 (m, 4H, C_6H_4); 5.43, 5.29 (s, 10 H, Cp); 4.69 (s, 1 H, C^2H); 4.06, 3.48 (s, 6 H, NMe_2). $^{13}C\{^1H\}$ NMR (acetone-d_6): δ/ppm = 256.0 (μ-CO); 224.8 (C^1); 210.0 (CO); 202.0 (C^3); 161.6 (d, $^1J_{CF}$ = 245 Hz, CF), 152.6, 129.7, 115.0 (d, $^2J_{CF}$ = 20.7 Hz) (C_6H_4); 121.4 (q, $^1J_{CF}$ = 320 Hz, CF_3); 91.7, 88.0 (Cp); 53.3 (C^2); 51.3, 44.4 (NMe_2). $^{19}F\{^1H\}$ NMR (acetone-d_6): δ/ppm = −112.3 (CF_3SO_3); −116.0 (C_6H_4F).

[$Fe_2Cp_2(CO)(\mu\text{-}CO)\{\mu\text{-}\eta^1\text{:}\eta^3\text{-}C^3(2\text{-}C_6H_4NH_2)C^2HC^1NMe_2\}$]$CF_3SO_3$, [4b]$CF_3SO_3$ (Chart 9).

Chart 9. Structure of [**4b**]$^+$.

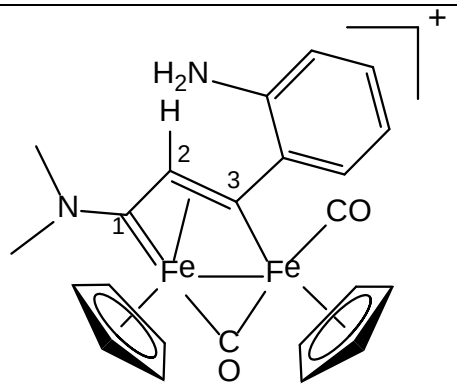

From [**2**]CF_3SO_3 and 2-ethynylaniline. Brown solid, yield 84%. Anal. calcd. for $C_{24}H_{23}F_3Fe_2N_2O_5S$: C, 46.48; H, 3.74; N, 4.52. Found: C, 46.30; H, 3.81; N, 4.40. IR (CH_2Cl_2): ũ/cm^{-1} = 1984vs (CO), 1809s (μ-CO), 1685m (C^2C^1N). ^{1}H NMR (acetone-d_6): δ/ppm = 7.78, 7.19, 7.05, 6.94 (m, 4 H, $C_6H_4NH_2$); 5.46, 5.18 (s, 10 H, Cp); 4.62 (s, 1 H, C^2H); 4.40 (br, 2 H, NH_2); 4.02, 3.42 (s, 6 H, NMe_2). $^{13}C\{^1H\}$ NMR (acetone-d_6): δ/ppm = 255.7 (μ-CO); 225.1 (C^1); 211.0 (CO); 203.2 (C^3); 141.9, 141.2, 128.1, 127.7, 117.7, 116.1 (C_6H_4); 91.9, 87.9 (Cp); 54.6 (C^2); 51.3, 44.3 (NMe_2).

[Fe_2Cp_2(CO)(μ-CO){μ-η^1:η^3-C^3(4-C_6H_4Me)$C^2HC^1NMe_2$}]CF_3SO_3, [4c]CF_3SO_3 (Chart 10).[19a]

Chart 10. Structure of [**4c**]$^+$.

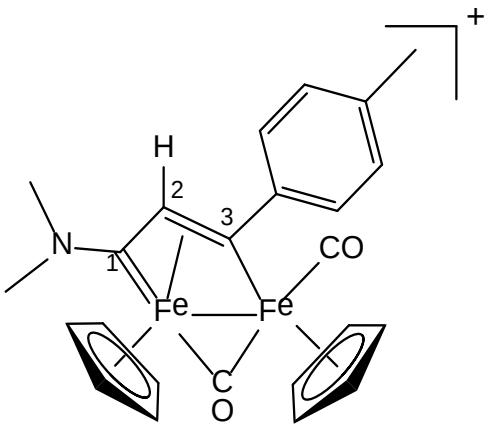

From [**2**]CF_3SO_3 and 4-ethynyltoluene. Brown solid, yield 88%. Anal. calcd. for $C_{25}H_{24}F_3Fe_2NO_5S$: C, 48.49; H, 3.91; N, 2.26. Found: C, 48.31; H, 3.96; N, 2.20. IR (CH_2Cl_2): ũ/cm^{-1} = 1992vs (CO), 1807s (μ-CO), 1684m (C^2C^1N). ^{1}H NMR (acetone-d_6): δ/ppm = 7.66, 7.35 (d, $^3J_{HH}$ = 7.83 Hz, 4 H, C_6H_4Me); 5.33, 5.21 (s, 10 H, Cp); 4.50 (s, 1 H, C^2H); 3.85, 3.28 (s, 6 H, NMe_2); 2.43 (s, 3 H, C_6H_4Me). $^{13}C\{^1H\}$ NMR ($CDCl_3$): δ/ppm = 257.2 (μ-CO); 225.3 (C^1); 209.9 (CO); 204.6 (C^3); 153.3 (*ipso*-C_6H_4Me); 137.5, 129.4, 127.1 (C_6H_4Me); 91.1, 87.7 (Cp); 52.5 (C^2); 51.6, 44.5 (NMe_2); 21.0 (C_6H_4Me).

3) Synthesis and characterization of monoiron compounds. *General procedure*. The appropriate precursor, [**3-4**]CF_3SO_3 (ca. 0.7 mmol), was dissolved in tetrahydrofuran (ca. 20 mL), and the solution was treated with pyrrolidine (ca. 10 eq.). The resulting mixture was stirred at ambient temperature overnight, then it was filtered through a short alumina pad using acetonitrile as eluent. The filtrated solution was dried under vacuum. The residue was dissolved in diethyl ether/dichloromethane mixture and charged on an alumina column. Elution with petroleum ether/diethyl ether mixtures allowed to remove impurities, then the fraction corresponding to the product was collected. Removal of the volatiles under reduced pressure afforded an air stable solid. Yields are given with respect to C^1.

[FeCp(CO){C^1NMe(Xyl)C^2HC^3(4-C_6H_4F)C(=O)}], 5a (Chart 11).

Chart 11. Structure of **5a**.

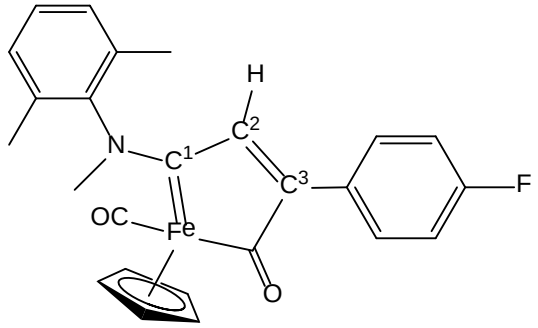

From [**3a**]CF_3SO_3. Brown solid, yield 63%. Eluent for chromatography: Et_2O. Anal. calcd. for $C_{25}H_{22}FFeNO_2$: C, 67.74; H, 5.00; N, 3.16. Found: C, 67.80; H, 4.91; N, 3.24. IR (CH_2Cl_2): ũ/cm^{-1} = 1920vs (CO), 1615s (CO_{acyl}), 1600s-sh (C^1N). IR (solid state): ũ/cm^{-1} = 3094vw, 3033w, 1900vs (CO), 1616m (CO_{acyl}), 1604m-sh (C^1N), 1591w-m, 1500m, 1491m-sh, 1471w-m, 1436m, 1392m, 1297w, 1239w-m, 1214m, 1161w-m, 1141w-m, 1086m, 1057w-m, 1052w-m, 1007w-m, 989m, 842s, 818s-sh, 810s, 773m-s, 747w-m, 734w-m, 709m, 653w-m. ^{1}H NMR (dmso-d_6): δ/ppm = 7.29, 7.12 (m, 7 H, C_6H_4 + $C_6H_3Me_2$); 6.80 (s, 1 H, C^2H); 4.72 (s, 5 H, Cp); 3.83 (s, 3 H, NMe); 2.23, 2.09 (s, 6 H, $C_6H_3Me_2$). $^{13}C\{^1H\}$ NMR (dmso-d_6): δ/ppm = 266.5 (CO_{acyl}); 262.5 (C^1); 222.4 (CO); 167.1 (C^3); 163.0 (d, $^1J_{CF}$ = 249 Hz, CF); 147.6 (C^2); 145.4 (*ipso*-$C_6H_3Me_2$); 132.8, 132.4, 129.5, 129.4, 129.2 ($C_6H_3Me_2$); 131.4 (d, $^3J_{CF}$ = 7.5 Hz), 115.6 (d, $^2J_{CF}$ = 20.7 Hz) (C_6H_4); 129.0 (*ipso*-C_6H_4); 85.7 (Cp); 49.5 (NMe); 17.7, 17.3 ($C_6H_3Me_2$). $^{19}F\{^1H\}$ NMR (DMSO-d_6): δ/ppm = −111.7. Crystals of **5a** suitable for X-ray analysis were obtained from a dichloromethane solution layered with pentane and stored at −30 °C.

[FeCp(CO){C^1NMe(Xyl)C^2HC^3(3-C_6H_4F)C(=O)}], 5b (Chart 12).

Chart 12. Structure of **5b**.

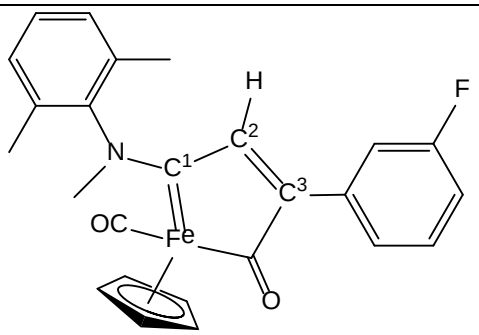

From [**3b**]CF_3SO_3. Brown solid, yield 70%. Eluent for chromatography: Et_2O/CH_2Cl_2 1:1 v/v. Anal. calcd. for $C_{25}H_{22}FFeNO_2$: C, 67.74; H, 5.00; N, 3.16. Found: C, 67.48; H, 5.04; N, 3.20. IR (CH_2Cl_2): $\tilde{\upsilon}/cm^{-1}$ = 1922vs (CO), 1640w-sh (CO_{acyl}), 1602s (C^1N), 1578m (arom C-C). IR (solid state): $\tilde{\upsilon}/cm^{-1}$ = 3079w, 3023w, 2923w, 1911vs (CO), 1638w (CO_{acyl}), 1601m (C^1N), 1575m, 1483s, 1473m, 1434w, 1389m, 1353w, 1294w, 1265m, 1241m, 1138w-m, 1079m, 1009m, 1001m, 895w, 875w-m, 812w, 802m, 779m-s, 741m, 712w, 683w-m, 657w. ^1H NMR ($CDCl_3$): δ/ppm = 7.28-7.12, 6.97 (m, 7 H, C_6H_4 + $C_6H_3Me_2$); 6.91 (s, 1 H, C^2H); 4.71 (s, 5 H, Cp); 3.87 (s, 3 H, NMe); 2.27, 2.15 (s, 6 H, $C_6H_3Me_2$). $^{13}C\{^1H\}$ NMR ($CDCl_3$): δ/ppm = 268.1 (CO_{acyl}); 265.5 (C^1); 221.2 (CO); 167.9 (C^3); 162.4 (d, $^1J_{CF}$ = 247 Hz, CF); 148.1 (C^2); 145.3 (*ipso*-$C_6H_3Me_2$); 134.5 (d, J_{CF} = 9.4 Hz), 132.5, 132.1, 129.5, 129.4, 129.1, 128.9, 124.8, 116.1 (d, J_{CF} = 22.6 Hz), 115.7 (d, J_{CF} = 20.7 Hz) ($C_6H_3Me_2$ + C_6H_4); 85.3 (Cp); 49.1 (NMe); 17.7, 17.5 ($C_6H_3Me_2$). $^{19}F\{^1H\}$ NMR (DMSO-d_6): δ/ppm = –113.3.

[FeCp(CO){C^1NMe(Xyl)C^2HC^3(2-C_6H_4F)C(=O)}], 5c (Chart 13).

Chart 13. Structure of **5c**.

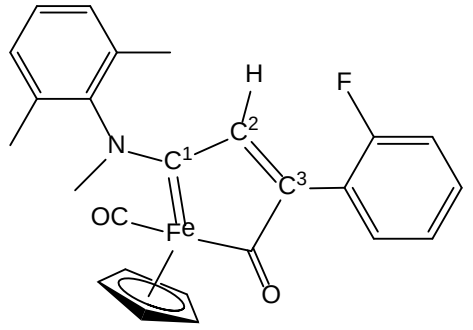

From [**3c**]CF_3SO_3. Brown solid, yield 70%. Eluent for chromatography: Et_2O/CH_2Cl_2 1:1 v/v. Anal. calcd. for $C_{25}H_{22}FFeNO_2$: C, 67.74; H, 5.00; N, 3.16. Found: C, 67.56; H, 5.05; N, 3.30. IR (CH_2Cl_2): $\tilde{\upsilon}/cm^{-1}$ = 1921vs (CO), 1619m (CO_{acyl}), 1605w-sh (C^1N). IR (solid state): $\tilde{\upsilon}/cm^{-1}$ = 3081vw, 2964vw, 2926vw, 1912vs (CO), 1617m (CO_{acyl}), 1608w-sh (C^1N), 1597w-m, 1575w, 1488m, 1472w-m, 1446w, 1432w, 1385w-m, 1257w-m, 1246w, 1211w, 1143w, 1083m, 985w-m, 885w, 815w-m, 784w-m, 766m, 747w-m, 707w, 657w. ^1H NMR (acetone-d_6): δ/ppm = 7.40, 7.26, 7.06 (m, 7 H, C_6H_4 +

$C_6H_3Me_2$); 7.28 (s, 1 H, C^2H); 4.75 (s, 5 H, Cp); 3.98 (s, 3 H, NMe); 2.31, 2.18 (s, 6 H, $C_6H_3Me_2$). $^{13}C\{^1H\}$ NMR (acetone-d_6): δ/ppm = 265.4 (CO_{acyl}); 262.9 (C^1); 221.7 (CO); 163.1 (C^3); 159.3 (d, $^1J_{CF}$ = 249 Hz, CF); 149.9 (C^2); 145.6 (*ipso*-$C_6H_3Me_2$); 132.5 (d, J_{CF} = 15.1 Hz), 132.0, 130.1 (d, J_{CF} = 7.5 Hz), 129.1, 129.0, 128.8, 123.5, 121.3 (d, J_{CF} = 13.2 Hz), 115.2 (d, J_{CF} = 22.6 Hz) (C_6H_4 + $C_6H_3Me_2$); 85.2 (Cp); 48.9 (NMe); 17.0, 16.7 ($C_6H_3Me_2$). $^{19}F\{^1H\}$ NMR (acetone-d_6): δ/ppm = –113.4.

[FeCp(CO){C^1NMe(Xyl)C^2HC^3(4-C_6H_4Me)C(=O)}], 5d (Chart 14).

Chart 14. Structure of **5d**.

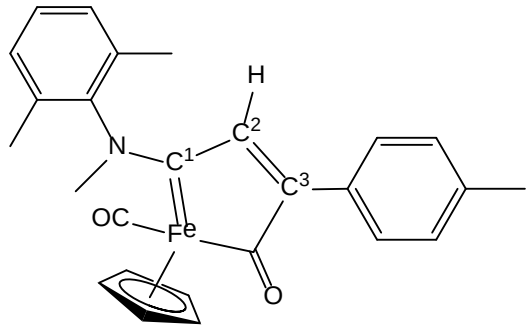

From [**5d**]CF_3SO_3. Brown solid, yield 62%. Eluent for chromatography: Et_2O/CH_2Cl_2 1:1 v/v. Anal. calcd. for $C_{26}H_{25}FeNO_2$: C, 71.08; H, 5.74; N, 3.19. Found: C, 70.71; H, 5.84; N, 3.22. IR (CH_2Cl_2): ũ/cm^{-1} = 1918vs (CO), 1614m-sh (CO_{acyl}), 1605m (C^1N). IR (solid state): ũ/cm^{-1} = 3023w, 2922w, 1906vs (CO), 1601br-s (C^1N + CO_{acyl}), 1489m, 1433w, 1387w, 1261w, 1241w, 1185w, 1140w, 1085s, 1021m, 992m, 884w, 808s, 742m, 720w, 654w. ^1H NMR ($CDCl_3$): δ/ppm = 7.28–7.25 (m), 7.22 (d, *J* = 7.4 Hz, 1H), 7.20–7.13 (m, 2H), 7.06 (d, *J* = 8.0 Hz, 2H) (C_6H_4Me + $C_6H_3Me_2$); 6.86 (s, 1H, C^2H); 4.68 (s, 5H, Cp); 3.85 (s, 3H, NMe); 2.28, 2.24, 2.12 (s, 9H, C_6H_4Me + $C_6H_3Me_2$). ^1H NMR (dmso-d_6): δ/ppm = 7.26-7.04 (m, 7 H, C_6H_4Me + $C_6H_3Me_2$); 6.77 (s, 1 H, C^2H); 4.70 (s, 5 H, Cp); 3.83 (s, 3 H, NMe); 2.24, 2.23, 2.08 (s, 9 H, C_6H_4Me + $C_6H_3Me_2$). $^{13}C\{^1H\}$ NMR ($CDCl_3$): δ/ppm = 268.7 (CO_{acyl}); 265.2 (C^1); 221.2 (CO); 169.5 (C^3); 146.9 (C^2); 145.3 (*ipso*-$C_6H_3Me_2$); 139.2, 132.6, 132.1, 129.6, 129.3, 129.0, 128.8, 128.7, 128.6 ($C_6H_3Me_2$); 85.1 (Cp); 48.8 (NMe); 21.3 (C_6H_4Me); 17.6, 17.4 ($C_6H_3Me_2$).

[FeCp(CO){C^1NMe(Xyl)C^2HC^3(3-C_6H_4Me)C(=O)}], 5e (Chart 15).

Chart 15. Structure of **5e**.

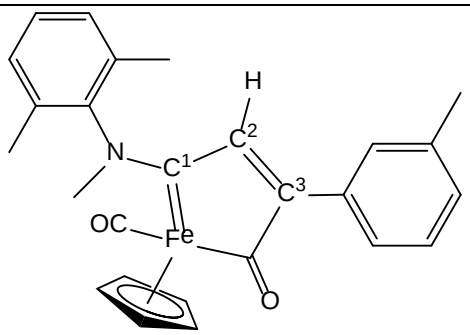

From [**3e**]CF_3SO_3. Brown solid, yield 68%. Eluent for chromatography: Et_2O/CH_2Cl_2 1:1 v/v. Anal. calcd. for $C_{26}H_{25}FeNO_2$: C, 71.08; H, 5.74; N, 3.19. Found: C, 70.56; H, 5.78; N, 3.16. IR (CH_2Cl_2): ũ/cm^{-1} = 1918vs (CO), 1623m (CO_{acyl}), 1605s (C^1N). IR (solid state): ũ/cm^{-1} = 3023w, 2922w, 1906vs (CO), 1601m-s (C^1N), 1489m, 1433w, 1387w, 1261w, 1241w, 1185w, 1140w, 1085s, 1021m, 992m, 884w, 808s, 742m, 720w, 654w. ^{1}H NMR (dmso-d_6): δ/ppm = 7.29-7.10 (m, 7 H, $C_6H_4Me + C_6H_3Me_2$); 6.90 (s, 1 H, C^2H); 4.71 (s, 5 H, Cp); 3.88 (s, 3 H, NMe); 2.31 (s, 3 H, C_6H_4Me); 2.27, 2.16 (s, 6H, $C_6H_3Me_2$). $^{13}C\{^1H\}$ NMR (dmso-d_6): δ/ppm = 268.6 (CO_{acyl}); 265.6 (C^1); 221.3 (CO); 169.9 (C^3); 147.6 (C^2); 145.4 (*ipso*-$C_6H_3Me_2$); 137.6, 132.7, 132.5, 132.2, 129.8, 129.4, 129.0, 128.7, 128.0, 126.1 ($C_6H_3Me_2$); 85.2 (Cp); 49.0 (NMe); 21.4 (C_6H_4Me); 17.7, 17.5 ($C_6H_3Me_2$).

[FeCp(CO){C^1NMe(Xyl)C^2HC^3(4-C_6H_4Ph)C(=O)}], 5f (Chart 16).

Chart 16. Structure of **5f**.

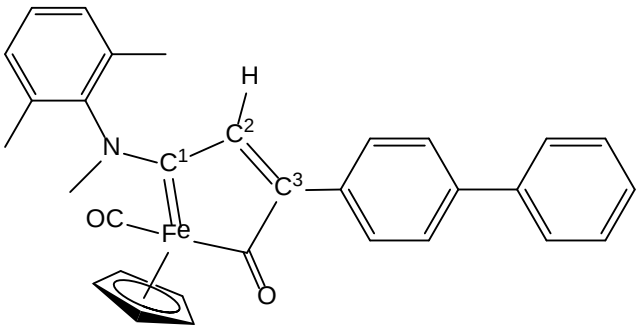

From [**3f**]CF_3SO_3. Brown solid, yield 58%. Eluent for chromatography: Et_2O. Anal. calcd. for $C_{31}H_{27}FeNO_2$: C, 74.26; H, 5.43; N, 2.79. Found: C, 74.05; H, 5.56; N, 2.61. IR (CH_2Cl_2): ũ/cm^{-1} = 1918vs (CO), 1610m (CO_{acyl}), 1599w (C^1N). IR (solid state): ũ/cm^{-1} = 2964vw, 1919vs (CO), 1610m-sh (CO_{acyl}), 1592s (C^1N), 1445s, 1430w-m, 1387m, 1261m, 1237m, 1141m, 1086m, 1029m, 991m, 916w, 883w-m, 841m, 808m-s, 769m-s, 735m, 715m, 698m, 654w-m. ^{1}H NMR ($CDCl_3$): δ/ppm = 7.56-7.21 (m, 12 H, $C_{12}H_9 + C_6H_3Me_2$); 6.96 (s, 1 H, C^2H); 4.73 (s, 5 H, Cp); 3.89 (s, 3 H, NMe); 2.28, 2.17 (s, 6 H; $C_6H_3Me_2$). $^{13}C\{^1H\}$ NMR (dmso-d_6): δ/ppm = 266.4 (CO_{acyl}); 262.5 (C^1); 222.5 (CO); 168.0 (C^3); 147.5 (C^2); 145.5 (*ipso*-$C_6H_3Me_2$); 141.1, 139.9, 132.8, 132.4, 131.7, 129.7, 129.5, 129.4, 129.2, 128.2, 127.1, 126.9, 125.4 ($C_{12}H_9 + C_6H_3Me_2$); 85.7 (Cp); 49.5 (NMe); 17.7, 17.3 ($C_6H_3Me_2$).

[FeCp(CO){C^1NMe(Xyl)C^2HC^3(2-$C_6H_4NH_2$)C(=O)}], 5g (Chart 17).

Chart 17. Structure of **5g**.

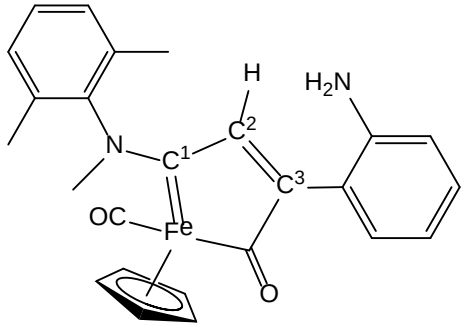

From [**3g**]CF_3SO_3. Brown solid, yield 81%. Eluent for chromatography: CH_2Cl_2. Anal. calcd. for $C_{25}H_{24}FeN_2O_2$: C, 68.19; H, 5.49; N, 6.36. Found: C, 67.74; H, 5.36; N, 6.41. IR (CH_2Cl_2): ũ/cm^{-1} = 1927vs (CO), 1614m (CO_{acyl}), 1603m (C^1N), 1581m (arom C-C). IR (solid state): ũ/cm^{-1} = 3319w (NH_2), 2965w, 1904s (CO), 1614m (CO_{acyl}), 1599m-sh (C^1N), 1589m, 1486m, 1390m, 1261m, 1088s, 1019s, 983m, 799vs, 770s, 751m, 668m. ^{1}H NMR ($CDCl_3$): δ/ppm = 7.28-7.06 (m, 7 H, $C_6H_4NH_2$ + $C_6H_3Me_2$); *7.73*, 6.85 (s, 1 H, C^2H); 4.72 (s, 5 H, Cp); 4.06 (s, 2 H, NH_2); 3.86, *3.68* (s, 3 H, NMe); *2.45*, *2.39*, 2.25, 2.17 (s, 6 H; $C_6H_3Me_2$). E/Z ratio = 5. $^{13}C\{^1H\}$ NMR ($CDCl_3$): δ/ppm = 271.8, *270.0* (CO_{acyl}); 265.2, *262.8* (C^1); *224.6*, 221.3 (CO); 173.5, *171.0* (C^3); 150.2 (C^2); *149.3*, 149.0, 141.1, *134.0, 133.2*, 132.5, 132.0, 130.2, 129.4, 129.3, 129.2, 129.0, 128.8, 128.2, *121.9*, 121.3, *118.2*, 118.0, 117.0 ($C_6H_4NH_2$ + $C_6H_3Me_2$); 145.6, *145.3* (*ipso*-$C_6H_3Me_2$); *85.7*, 85.2 (Cp); 49.0, *44.7* (NMe); *18.5*, 17.7, 17.5 ($C_6H_3Me_2$).

[FeCp(CO){C^1NMe(Xyl)C^2HC^3(3-C_6H_4OH)C(=O)}], 5h (Chart 18).

Chart 18. Structure of **5h**.

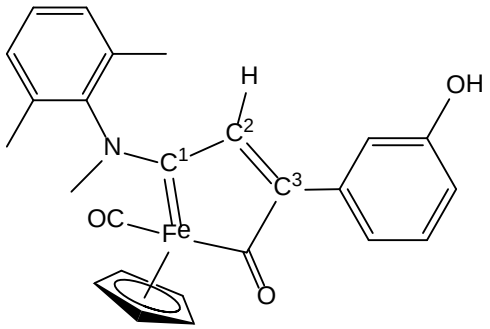

From [**4h**]CF_3SO_3. Brown solid, yield 84%. Eluent for chromatography: CH_2Cl_2/MeOH 9:1 v/v. Anal. calcd. for $C_{25}H_{23}FeNO_3$: C, 68.04; H, 5.25; N, 3.17. Found: C, 67.63; H, 5.33; N, 3.06. IR (CH_2Cl_2): ũ/cm^{-1} = 1925vs (CO), 1664m (CO_{acyl}), 1599m (C^1N), 1574s (arom C-C). IR (solid state): ũ/cm^{-1} = 3139w-br (OH), 3023vw, 1944m, 1922vs (CO), 1653w (CO_{acyl}), 1554m, 1490m, 1471w-m, 1436m, 1390m, 1301m,1275w-m, 1232m, 1200w-m, 1140w-m, 1080w-m, 1047w-m, 1013m, 908w-m, 875w-m, 842w-m, 820m, 773w-m, 750m, 720m, 692w-m,

657w-m. ^{1}H NMR ($CDCl_3$): δ/ppm = 7.61 (s, 1 H, arom CH); 7.27-7.10 (m, 3 H, arom CH); 6.97 (s, 1 H, C^2H); 6.90 (br, 1 H, OH); 4.71 (s, 5 H, Cp); 3.87 (s, 3 H, NMe); 2.28, 2.12 (s, 6 H, $C_6H_3\mathit{Me}_2$). $^{13}C\{^{1}H\}$ NMR ($CDCl_3$): δ/ppm = 276.6 (CO_{acyl}); 265.5 (C^1); 220.9 (CO); 170.1 (C^3); 157.1 (*ipso*-C_6H_4OH); 148.3 (C^2); 145.1 (*ipso*-$\mathit{C}_6H_3Me_2$); 133.3, 132.8, 132.0, 129.5, 129.2, 129.0, 128.8, 119.7 (C_6H_4OH + $\mathit{C}_6H_3Me_2$); 85.0 (Cp); 49.1 (NMe); 17.7, 17.4 ($C_6H_3\mathit{Me}_2$). Crystals of **5h** suitable for X-ray analysis were collected from a dichloromethane solution layered with pentane and stored at −30 °C.

[FeCp(CO){C^1N(Me)$_2$$C^2HC^3$(4-$C_6H_4F$)C(=O)}], 6a (Chart 19).

Chart 19. Structure of **6a**.

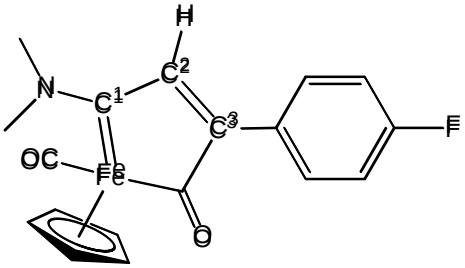

From [**4a**]CF_3SO_3. Brown solid, yield 55%. Eluent for chromatography: CH_2Cl_2. Anal. calcd. for $C_{18}H_{16}FFeNO_2$: C, 61.22; H, 4.57; N, 3.97. Found: C, 61.01; H, 4.66; N, 3.80. IR (CH_2Cl_2): ũ/cm^{-1} = 1916vs (CO), 1619m (CO_{acyl}), 1598s (C^1N). ^{1}H NMR (dmso-d_6): δ/ppm = 8.03 (s, 1 H, C^2H); 7.66, 7.20 (m, 4 H, C_6H_4F); 4.53 (s, 5 H, Cp); 3.68, 3.60 (s, 6 H, NMe_2). $^{13}C\{^{1}H\}$ NMR (dmso-d_6): δ/ppm = 269.0 (CO_{acyl}); 256.4 (C^1); 223.0 (CO); 166.2 (C^3); 162.8 (d, $^{1}J_{CF}$ = 247 Hz, CF); 148.2 (C^2); 131.8 (d, J_{CF} = 7.5 Hz), 115.3 (d, J_{CF} = 22.6 Hz) (C_6H_4F); 129.6 (*ipso*-C_6H_4), 85.4 (Cp); 51.9, 44.1 (NMe_2). $^{19}F\{^{1}H\}$ NMR (dmso-d_6): δ/ppm = −112.3.

[FeCp(CO){C^1N(Me)$_2$$C^2HC^3$(2-$C_6H_4NH_2$)C(=O)}], 6b (Chart 20).

Chart 20. Structure of **6b**.

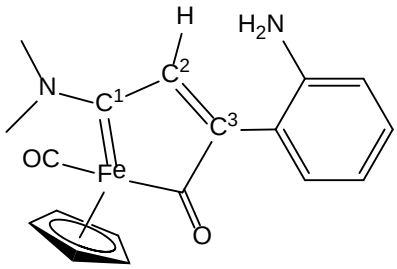

From [**4b**]CF_3SO_3. Brown solid, yield 30%. Eluent for chromatography: CH_2Cl_2/THF 1:1 v/v. Anal. calcd. for $C_{18}H_{18}FeN_2O_2$: C, 61.74; H, 5.18; N, 8.00. Found: C, 61.36; H, 5.18; N, 7.91. IR (CH_2Cl_2): ũ/cm^{-1} = 1918vs (CO), 1601m (CO_{acyl}), 1579m (C^1N). IR (solid state): ũ/cm^{-1} = 3441w-m (NH), 3354w-m (NH), 1889vs, 1627m-sh, 1589m-sh, 1574s, 1531m, 1485m, 1450w, 1409m, 1235m, 1153m, 1087s, 999s, 936w, 863m, 799vs, 767s,

749vs, 718vs, 703s. ^{1}H NMR (dmso-d_6): δ/ppm = 7.85 (s, 1 H, C^2H); 7.02 (t), 6.88 (d), 6.68 (d), 6.53 (t) (4 H, $C_6H_4NH_2$); 4.81 (s, 2 H, NH_2); 4.54 (s, 5 H, Cp); 3.69, 3.56 (s, 6 H, NMe_2). $^{13}C\{^1H\}$ NMR (dmso-d_6): δ/ppm = 270.9 (CO_{acyl}); 256.6 (C^1); 223.1 (CO); 170.6 (C^3); 149.4 (C^2); 146.9, 130.8, 129.6, 120.3, 116.3, 116.1 (C_6H_4); 85.4 (Cp); 51.8, 44.0 (NMe_2). Crystallization from a dichloromethane solution layered with pentane and stored at −30 °C afforded dark brown crystals of **6b** suitable for X-ray analysis.

4) X-ray crystallography.

Crystal data and collection details for **5a**, **5h·solv** and **6b·CH_2Cl_2** are reported in Table 5. Data were recorded on a Bruker APEX II diffractometer equipped with a PHOTON100 detector using Mo–Kα radiation. Data were corrected for Lorentz polarization and absorption effects (empirical absorption correction SADABS).[36] The structures were solved by direct methods and refined by full-matrix least-squares based on all data using F^2.[37] Hydrogen atoms were fixed at calculated positions and refined by a riding model, except otherwise stated. All non-hydrogen atoms were refined with anisotropic displacement parameters. The crystals of **5a** appeared to be racemically twinned with refined batch factor 0.07(3). The crystals of **5h·solv** contained some solvent accessible voids which were treated with the SQUEEZE routine of PLATON.[38] Two independent molecules with similar geometries and bonding parameters are present within the unit cell of **5h·solv.** The O-bonded H-atoms of **5h·solv** were preliminarily located in the Fourier Difference Map and, then, refined by a riding model. The C, N and O atoms of **5h·solv** were restrained to have similar thermal parameters (SIMU line in SHELXL, s.u. 0.01). The N-bonded H-atoms of **6b·CH_2Cl_2** were located in the Fourier Difference Map and refined isotropically, using the 1.2-fold U_{eq} value of the parent atoms.

Table 5. Crystal data and measurement details for **5a**, **5h** and **6b**.

	5a	**5h·solv**	**6b·CH_2Cl_2**
Formula	$C_{25}H_{22}FFeNO_2$	$C_{25}H_{23}FeNO_3$	$C_{19}H_{20}Cl_2FeN_2O_2$
FW	443.28	441.29	435.12
T, K	293(2)	293(2)	293(2)
λ, Å	0.71073	0.71073	0.71073
Crystal system	Monoclinic	Trigonal	Orthorhombic
Space group	*Cc*	$R\bar{3}$	*Pbca*
a, Å	11.344(2)	36.712(3)	21.588(2)
b, Å	25.609(5)	36.712(3)	7.7569(9)
c, Å	8.5284(15)	20.4924(16)	22.950(3)
β,°	121.802(5)	90	90
Cell Volume, Å^3	2105.7(7)	23919(4)	3843.2(8)
Z	4	36	2
D_c, g·cm^{-3}	1.398	1.103	1.504

μ, mm^{-1}	0.746	0.588	1.079
F(000)	920	8280	1792
Crystal size, mm	0.16×0.13×0.11	0.21×0.15×0.12	0.14×0.12×0.11
θ limits,°	2.257-24.993	1.922-25.000	1.887-25.497
Reflections collected	12553	49136	45015
Independent reflections	3705 [R_{int} = 0.0572]	9353 [R_{int} = 0.1743]	3571 [R_{int} = 0.0822]
Data / restraints /parameters	3705 / 2 / 275	9353 / 348 / 543	3571 / 2 / 243
Goodness on fit on F^2	1.066	1.048	1.120
R_1 (I > 2σ(I))	0.0437	0.1072	0.0826
wR_2 (all data)	0.0998	0.2405	0.2203
Largest diff. peak and hole, e $Å^{-3}$	0.651 / –0.316	0.653 / –0.370	0.970 / –1.119

5) Cell Culture and antiproliferative activity.

A2780, A2880cisR and HEK-293 cells were obtained from the European Collection of Cell Cultures (EACC). The human embryonic kidney cells (HEK-293) were cultured in DMEM medium supplemented with 2mM of Glutamine and 1% of nonessential amino acids (NEAA), whereas the ovarian carcinoma cells were cultured in RPMI-1640 medium supplemented with 2mM of Glutamine. All culture media were supplemented with 10% of 10% newborn calf serum and 1% amphotericin-penicillin-streptomycin solution. A270cisR cell line was incubated in the presence of 2 μM cisplatin every two passages. The antiproliferative activity was evaluated by the MTT Assay. Cells were seeded in 96-well plates at a density of 1×10^4 cells per well and incubated for 24h at 37 °C under 5% CO_2 atmosphere. Then, cells were treated with different concentrations of the complexes under study and cisplatin as a positive control. Since DMSO was employed to dissolve the iron complexes, a vehicle control with DMSO at the maximal concentration employed (0.5%) was also included. After 72 hours of incubation, cells were incubated with 100 μl of MTT (3-(4,5-dimethyltiazol-2-yl)-2,5-diphenyltetrazoliumbromide) (Merck) dissolved in culture medium (500 μg/ml) for 3 hours. Then, the formazan crystals were dissolved with 100 μL of solution (10% SDS and 0.01M HCl). After 18 hours of incubation, absorbance was read at 590 nm in a microplate reader (Cytation 5 Cell Imaging Multi-Mode Reader (Biotek Instruments, USA). Two independent experiments were performed with four replicates per dose. The IC_{50} values were calculated using GraphPadPrism Software Inc. (version 6.01, USA).

6) Bacterial strains and antibacterial activity.

Four different strains of pathogenic bacteria, i.e. *E. faecium* CECT 5253 (vancomycin resistant, Gram positive bacteria), *S. aureus* CECT 5190 (methicillin resistant, Gram positive bacteria), *A. baumannii* ATCC 17978 (Gram negative bacteria) and *P. aeruginosa* PAO1 (Gram negative bacteria), were used in this work. *A. baumannii*, *P. aeruginosa* and *S. aureus* strains were maintained at 37 ºC in Mueller-Hinton (MH) broth or agar while *E. faecium* was maintained in Tryptic Soy (TS) broth or agar at 37 ºC. To test the antibacterial activity, the broth microdilution plate method according to CLSI criteria against ESKAPE (*Enteroccocus faecium, Staphylococcus aureus, Klebsiella pneumoniae, Acinetobacter baumannii, Pseudomonas aeruginosa*, and *Enterobacter cloacae*) pathogens was employed.[39] Briefly, serial dilutions of the compounds were prepared in MHB ranging from 100 µM to 3.1 µM (1:2 dilutions) in 96-well plates. Inoculated plates with a final concentration of 5×10^5 CFU/mL were incubated at 37 ºC for 18-20 hours. The reported Minimum Inhibitory concentrations (MIC) are the mean values from at least two independent experiments with three replicates.

7) Stability studies in aqueous media.

A) Stability in dmso/water. A mixture of the selected Fe compound (**[3a]**CF_3SO_3, **5a**, **5e**, **5g**, **5h** *ca*. 3 mg), dmso-d_6 (0.4 mL) and a D_2O solution (0.3 mL; 0.2 mL for **5e**) containing Me_2SO_2 ($3.36\cdot10^{-3}$ M) was stirred for 30 minutes then filtered over celite and transferred into an NMR tube. The resulting orange-brown solution was analyzed by ^1H and ^{19}F NMR then heated at 37 °C for 48 hours. After cooling to room temperature, the solution was filtered over celite and NMR analyses were repeated. The amount of starting material (% with respect to the initial spectrum) was calculated by the relative integral with respect to Me_2SO_2 as internal standard[40] (δ/ppm = 2.95 (s, 6H)) (Table S1). NMR data for the tested compounds are given in the SI; ^1H chemical shifts are referenced to the dmso-d_5 signal as in pure dmso-d_6 (δ/ppm = 2.50).

B) Stability in dmso/cell culture medium. Powdered DMEM cell culture medium (1000 mg/L glucose and L-glutamine, without sodium bicarbonate and phenol red; D2902 - Sigma Aldrich) was dissolved in D_2O (10 mg/mL), according to the manifacturer's instructions. The solution of deuterated cell culture medium ("DMEM-d") was treated with Me_2SO_2 ($6.6\cdot10^{-3}$ M) and NaH_2PO_4 / Na_2HPO_4 (0.15 M, pD = 7.5[41]), then stored at 4 °C under N_2. The selected Fe compound (*ca*. 4 mg) was suspended in a solution containing dmso-d_6 and DMEM-d (2:1 *v*/*v* for **[3a]**CF_3SO_3, **5g**, **5h;** 3:1 *v*/*v* for **5a**, **5e**). The mixture was stirred for 30 minutes then filtered over celite and transferred into an NMR tube. The resulting orange-brown solution was analyzed by ^1H and ^{19}F NMR then heated at 37 °C for 24 hours. After cooling to room temperature, the solution was filtered over celite and NMR analyses were repeated. The amount of starting material (% with respect to the initial spectrum) was calculated by the relative integral with respect to Me_2SO_2 as internal standard[40] (δ/ppm = 2.95 (s, 6H)) (Table S1).

C) Carbon monoxide release. In a 15x45 cm screw top vial (4.80 mL total volume), the selected Fe compound (**[3a]**CF_3SO_3, **5a**, **5e**, **5g**, **5h**; n_{Fe} *ca*. 6-9·10^{-3} mmol), was dissolved in DMSO then diluted with RMPI-1640 cell culture medium (3.70 mL total liquid volume; 2:1 *v*/*v*). The mixture was sealed with screw caps with PTFE septa and heated at 37 °C for 24 hours under stirring. After 24 hours, the headspace (1.10 mL) was sampled with a gastight microsyringe (250 μL) and analyzed by GC-TCD. The amount of carbon monoxide released (n_{CO}, mmol) was calculated on the basis of a calibration curve built using air/carbon monoxide mixtures (2.0 – 18 % *v*/*v*). The number of equivalents of carbon monoxide released were calculated with respect to the initial amount of iron compound (eq_{CO} = n_{CO}/n_{Fe}). The related amount of starting material was calculated on the basis of the equivalents of CO released, by assuming the release of 2 eq. of CO for each Fe compound (% starting material = [1 - $eq_{CO}/2$]·100). Data is reported in Table 6.

Table 6. Release of CO (number of equivalents) as determined by GC-TCD analysis and stability of selected Fe compounds in dmso/cell culture medium 2:1 *v*/*v* mixtures after 24 hours at 37 °C.

Compound	eq. CO released [a]	% starting material [b]
[3a]CF_3SO_3	0.5	*ca*. 75%
5a	0.4	*ca*. 80%
5e	0.5	*ca*. 75%
5g	0.5	*ca*. 75%
5h	0.4	*ca*. 80%

[a] $eq_{CO} = n_{CO}/n_{Fe}$; [b] % starting material = [1 - $eq_{CO}/2$]•100

8) Catalytic NADH oxidation

NADH was stored at –20 °C under N_2; a stock NADH solution (2.3·10^{-4} mol·L^{-1}) was prepared in phosphate buffered aqueous solution (Na_2HPO_4/NaH_2PO_4; 5.5·10^{-3} mol·L^{-1}, pH = 7.2) and stored at 4 °C. Stock solutions of Fe compounds (**[3a]**CF_3SO_3, **5a**, **5e**, **5g**, **5h**; 2.0·10^{-4} mol·L^{-1}) were prepared in DMSO immediately before use. $FeSO_4$ was used as a reference compounds (stock solution prepared in H_2O). Solutions of each iron compound (0.35 mL) and NADH (6.6 mL) were mixed, resulting in a 5 % DMSO aqueous solution containing 2.2·10^{-4} M NADH and 1.0·10^{-5} M iron compound (4.5 % mol/mol). The solution was stirred at 37 °C for 24 hours and periodically analyzed by UV-Vis spectroscopy (260-460 nm) using PMMA cuvettes (1.0 cm path-length). Turnover numbers were calculated as TON = c(0)/c_{Fe}·[A(0) - A(t)]/A(0) where A is the absorbance at λ_{max} = 339 nm; c(0) and c_{Fe} are the initial molar concentrations of NADH and the selected Fe compound, respectively (Table 3).

Acknowledgements

We gratefully thank the University of Pisa (Fondi di Ateneo 2019), the Caixa Foundation (LCF/PR/PR12/11070003), the Ministerio de Ciencia, Innovación y Universidades (RTI2018-102040-B-100) and the Junta de Castilla y León (BU305P18, FEDER Funds) for funding.

Supporting Information Available

NMR spectra of products. CCDC reference numbers XXXX (**5a**), XXXX (**5h**) and XXXX (**6b**) contain the supplementary crystallographic data for the X-ray studies reported in this paper. These data can be obtained free of charge at www.ccdc.cam.ac.uk/conts/retrieving.html (or from the Cambridge Crystallographic Data Centre, 12, Union Road, Cambridge CB2 1EZ, UK; fax: (internat.) +44-1223/336-033; e-mail: deposit@ccdc.cam.ac.uk).

References

1 (a) M. Sánchez, L. Sabio, N. Gálvez, M. Capdevila, J. M. Dominguez-Vera, IUBMB Life, 2017, 69, 382-388. (b) I. Bratsos, T. Gianferrara, E. Alessio, C. G. Hartinger, M. A. Jakupec, B. K. Keppler, Essential Metal Related Metabolic Disorders, in Bioinorganic Medicinal Chemistry, ed. E. Alessio, Wiley-VCH, Weinheim, 2011, 151-174. (c) A. Fürstner, ACS Cent. Sci. 2016, 2, 778-789. (d) T. Bleith, H. Wadepohl, L. H. Gade, J. Am. Chem. Soc. 2015, 137, 2456−2459.

2 (a) X. Jiang, L. Chen, X. Wang, L. Long, Z. Xiao, X. Liu, Chem. Eur. J. 2015, 21, 13065-13072. (b) D. Scapens, H. Adams, T. R. Johnson, B. E. Mann, P. Sawle, R. Aqil, T. Perrior, R. Motterlini, Dalton Trans. 2007, 4962–4973. (c) L. Hewison, S. H. Crook, T. R. Johnson, B. E. Mann, H. Adams, S. E. Plant, P. Sawle, R. Motterlini, Dalton Trans. 2010, 39, 8967–8975.

3 (a) A. J. Atkin, I. J. S. Fairlamb, J. S. Ward, J. M. Lynam, Organometallics 2012, 31, 5894−5902. (b) S. Romanski, H. Rücker, E. Stamellou, M. Guttentag, J.-M. Neudörfl, R. Alberto, S. Amslinger, B. Yard, H.-G. Schmalz, Organometallics 2012, 31, 5800-5809. (c) N. S. Sitnikov, Y. Li, D. Zhang, B. Yard, H.-G. Schmalz, Angew. Chem. Int. Ed. 2015, 54, 12314 –12318. (d) L. Hewison, S. H. Crook, B. E. Mann, A. J. H. M. Meijer, H. Adams, P. Sawle, R. A. Motterlini, Organometallics 2012, 31, 5823-5834.

4 (a) Z. Xiao, R. Jiang, J. Jin, X. Yang, B. Xu, X. Liu, Y. He, Y. He, Dalton Trans. 2019, 48, 468–477. (b) X. Jiang, L. Long, H. Wang, L. Chen, X. Liu, Dalton Trans. 2014, 43, 9968–9975.

5 (a) K. Ling, F. Men, W.-C. Wang, Y.-Q. Zhou, H.-W. Zhang, D.-W. Ye, J. Med. Chem. 2018, 61, 2611-2635. (b) S. H. Heinemann, T. Hoshi, M. Westerhausen, A. Schiller, Chem. Commun., 2014, 50, 3644-3660.

6 (a) C. Hirschhäuser, J. Velcicky, D. Schlawe, E. Hessler, A. Majdalani, J.-M. Neudçrfl, A. Prokop, T. Wieder, H.-G. Schmalz, Chem. Eur. J. 2013, 19, 13017-13029. (b) A. Cingolani, V. Zanotti, S. Zacchini, M. Massi, P. V. Simpson, N. Maheshkumar Desai, I. Casari, M. Falasca, R. Rigamonti, R. Mazzoni, Appl. Organomet. Chem. 2019, 33, e4779. (c) C. Prinz, E. Vasyutina, G. Lohmann, A. Schrader, S. Romanski, C. Hirschhäuser, P. Mayer, C. Frias, C. D. Herling, M. Hallek, H.-G. Schmalz, A. Prokop, D. Mougiakakos, M. Herling, Molecular Cancer 2015, 14, 114. (d) J. C. Franke, M. Plötz, A. Prokop, C. C. Geilen, H.-G. Schmalz, J. Eberle, Biochem. Pharmacol. 2010, 79, 575–586.

7 (a) D. Astruc, Eur. J. Inorg. Chem. 2017, 6–29. (b) M. Patra, G. Gasser, Nat. Rev. 2017, 1, 1-11. (c) G. Jaouen, A. Vessieres, S. Top, Chem. Soc. Rev., 2015, 44, 8802—8817. (d) A. Singh, I. Lumb, V. Mehra, V. Kumar, Dalton Trans., 2019, 48 , 2840–2860.

8 b) P. R. Florindo, D. M. Pereira, P. M. Borralho, C. M. P. Rodrigues, M. F. M. Piedade, A. C. Fernandes, J. Med. Chem. 2015, 58, 4339-4347. b) A. Valente, A. M. Santos, L. Côrte-Real, M. P. Robalo, V. Moreno, M. Font-Bardia, T. Calvet, J. Lorenzo, M. H. Garcia, J. Organomet. Chem. 2014, 756, 52-60. c) A. C. Gonçalves, T. S. Morais, M. P. Robalo, F. Marques, F. Avecilla, C. P. Matos, I. Santos, A. I. Tomaz, M. H. Garcia, J. Inorg. Biochem. 2013, 129, 1–8.

9 R. H. Crabtree, The Organometallic Chemistry of the Transition Metals, Wiley Ed., 2014.

10 A. Pilon, P. Gírio, G. Nogueira, F. Avecilla, H. Adams, J. Lorenzo, M. H. Garcia, A. Valente, J. Organomet. Chem. 2017, 852, 34-42.

11 G. Agonigi, L. Biancalana, M. G. Lupo, M. Montopoli, N. Ferri, S. Zacchini, F. Binacchi, T. Biver, B. Campanella, G. Pampaloni, V. Zanotti, F. Marchetti, Organometallics 2020, 39, 645-657.

12 (a) S. Gao, Y. Liu, Y. Shao, D. Jiang, Q. Duan, Coord. Chem. Rev. 2020, 402, 213081. (b) Y. Li, T. B. Rauchfuss, Chem. Rev. 2016, 116, 7043-7077. (c) S. I. Kalläne, A. W. Hahn, T. Weyherm※ller, E. Bill, F. Neese, S. DeBeer, M. van Gastel, Inorg. Chem. 2019, 58, 5111−5125. (d) F. Arrigoni, L. Bertini, L. De Gioia, A. Cingolani, R. Mazzoni, V. Zanotti, G. Zampella, Inorg. Chem. 2017, 56, 13852-13864.

13 Recent reviews: (a) F. Marchetti, Eur. J. Inorg. Chem. 2018, 3987–4003, and references therein. (b) R. Mazzoni, F. Marchetti, A. Cingolani, V. Zanotti, Inorganics 2019, 7, 25; doi:10.3390/inorganics7030025, and references therein.

14 See for instance: a) F. Marchetti, S. Zacchini, V. Zanotti, Organometallics 2016, 35, 2630−2637. b) M. A. Alvarez, M. E. García, R. González, M. A. Ruiz, Organometallics 2013, 32, 4601-4611. c) A. Boni, T. Funaioli, F. Marchetti, G. Pampaloni, C. Pinzino, S. Zacchini, Organometallics 2011, 30, 4115-4122. d) C. P. Casey, E. A. Austin, J. Am. Chem. Soc. 1988, 110, 7106-7113. e) M. Etienne, J. Talarmin, L. Toupets, Organometallics 1992, 11, 2058-2068. f) S. Doherty, M. R. J. Elsegood, W. Clegg, M. F. Ward, M. Waugh, Organometallics 1997, 16, 4251-4253.

15 (a) P. Zimmer, Y. Sun, W. R. Thiel, J. Organomet. Chem. 2014, 774, 12-18. (b) N. J. Coville, E. A. Darling, A. W. Hearn, P. Johnston, J. Organomet. Chem. 1987, 328, 375-385. (c) W. E. Williams, F. J. Lalor, J. Chem. Soc., Dalton Trans. 1973, 13, 1329-1332. (d) J. Klösener, M. Wiesemann, B. Neumann, H.-G. Stammler, B. Hoge, Eur. J. Inorg. Chem. 2018, 3971–3977.

16 (a) E. J. Crawford, T. W. Bodnar, A. R. Cutler, J. Am. Chem. Soc. 1986, 108, 6202-6212. (b) L. H. Gade, H. Memmler, U. Kauper, A. Schneider, S. Fabre, I. Bezougli, M. Lutz, C. Galka, I. J. Scowen, M.

McPartlin, Chem. Eur. J. 2000, 6, 692-708. (c) N. Murshid, A. El-Temtamy, X. Wang, J. Organomet. Chem. 2017, 851, 40-45.

17 C. P. Casey, S. R. Marder, R. E. Colborn, P. A. Goodson, Organometallics 1986, 5, 199-203.

18 D. Rocco, L. K. Batchelor, G. Agonigi, S. Braccini, F. Chiellini, S. Schoch, T. Biver, T. Funaioli, S. Zacchini, L. Biancalana, M. Ruggeri, G. Pampaloni, P. J. Dyson, F. Marchetti, Chem. Eur. J. 2019, 25, 14801-14816.

19 a) V. G. Albano, L. Busetto, F. Marchetti, M. Monari, S. Zacchini and V. Zanotti, Organometallics, 2003, 22, 1326-1331. b) V. G. Albano, L. Busetto, F. Marchetti, M. Monari, S. Zacchini, V. Zanotti, J. Organomet. Chem., 2004, 689, 528–538. c) G. Ciancaleoni, S. Zacchini, V. Zanotti, F. Marchetti, Organometallics 2018, 37, 3718−3731.

20 a) L. Busetto, F. Marchetti, S. Zacchini, V. Zanotti, Organometallics 2005, 24, 2297-2306. b) L. Busetto, F. Marchetti, M. Salmi, S. Zacchini, V. Zanotti, Eur. J. Inorg. Chem. 2008, 2437–2447. c) F. Marchetti, S. Zacchini, V. Zanotti, Eur. J. Inorg. Chem. 2012, 2456–2463.

21 G. Agonigi, G. Ciancaleoni, T. Funaioli, S. Zacchini, F. Pineider, C. Pinzino,; G. Pampaloni, V. Zanotti, F. Marchetti, Inorg. Chem. 2018, 57, 15172−15186.

22 V. G. Albano, L. Busetto, F. Marchetti, M. Monari, S. Zacchini, V. Zanotti, J. Organomet. Chem. 2006, 691, 4234–4243.

23 D. Rocco, L. K. Batchelor, E. Ferretti, S. Zacchini, G. Pampaloni, P. J. Dyson, F. Marchetti, ChemPlusChem, ChemPlusChem 2020, 85, 110–122.

24 A. Frei, J. Zuegg, A. G. Elliott, M. Baker, S. Braese, C. Brown, F. Chen, C. G. Dowson, G. Dujardin, N. Jung, A. P. King, A. M. Mansour, M. Massi, J. Moat, H. A. Mohamed, A. K. Renfrew, P. J. Rutledge, P. J. Sadler, M. H. Todd, C. E. Willans, J. J. Wilson, M. A. Cooper, M. A. T. Blaskovich, Chem. Sci., 2020, 11 , 2627–2639.

25 G. Agonigi, M. Bortoluzzi, F. Marchetti, G. Pampaloni, S. Zacchini, V. Zanotti, Eur. J. Inorg. Chem. 2018, 960-971.

26 (a) I. Yu, C. J. Wallis, B. O. Patrick, P. L. Diaconescu, P. Mehrkhodavandi, Organometallics 2010, 29, 6065-6076. (b) S. G. Davies, A. J. Edwards, S. Jones, M. R. Metzler, K. Yanada, R. Yanada, J. Chem. Soc., Dalton Trans. 1998, 1587–1594. (c) H. Adams, N. A. Bailey, C. Ridgway, B. F. Taylor, S. J. Walters, M. J. J. Organomet. Chem. 1990, 394, 349-364. (d) J. Park, J. Kim, Organometallics 1995, 14, 4431-4434.

27 S. G. Eaves, D. S. Yufit, B. W. Skelton, J. A. K. Howard, P. J. Low, Dalton Trans. 2015, 44, 14341-14348.

28 Q. Du, L. Guo, M. Tian, X. Ge, Y. Yang, X. Jian, Z. Xu, Z. Tian, Z. Liu, Organometallics 2018, 37, 2880−2889.

29 F. Q. Schafer, G. R. Buettner, Free Rad. Biol. Med. 2011, 30, 1191–1212.

30 Y. Fu, M. J. Romero, A. Habtemariam, M. E. Snowden, L. Song, G. J. Clarkson, B. Qamar, A. M. Pizarro, P. R. Unwin, P. J. Sadler, Chem. Sci. 2012, 3, 2485-2493.

31 P. Marzenell, H. Hagen, L. Sellner, T. Zenz, R. Grinyte, V. Pavlov, S. Daum, A. Mokhir, J. Med. Chem. 2013, 56, 6935 − 6944.

32 F. Menges, "Spectragryph - optical spectroscopy software", Version 1.2.5, @ 2016-2017, http://www.effemm2.de/spectragryph.

33 Fulmer, G. R.; Miller, A. J. M.; Sherden, N. H.; Gottlieb, H. E.; Nudelman, A.; Stoltz, B. M.; Bercaw, J. E.; Goldberg, K. I. NMR Chemical Shifts of Trace Impurities: Common Laboratory Solvents, Organics, and Gases in Deuterated Solvents Relevant to the Organometallic Chemist, Organometallics 2010, 29, 2176–2179.

34 W. Willker, D. Leibfritz, R. Kerssebaum, and W. Bermel, Magn. Reson. Chem., 1993, 31, 287-292.

35 ^{1}H NMR (acetone-d_6): δ/ppm = 7.56, 7.18 (m, 4H); 3.65 (s, 1H). 19F NMR (acetone-d_6): δ/ppm = □111.9 (s).

36 G. M. Sheldrick, SADABS-2008/1 - Bruker AXS Area Detector Scaling and Absorption Correction, Bruker AXS: Madison, Wisconsin, USA, 2008

37 G. M. Sheldrick, ActaCrystallogr. C, 2015, 71, 3.

38 (a) A. L. Spek, PLATON, A Multipurpose Crystallographic Tool, Utrecht University, Utrecht, The Netherlands, 2005. (b) A. L. Spek, J. Appl. Crystallogr. 2003, 36, 7. (c) A. L. Spek, Acta Crystallogr. 2009, D65, 1.

39 Clinical and Laboratory Standards Institute. Performance standards for antimicrobial susceptibility testing: 17th informational supplement M07-A9. Clinical and Laboratory Standards Institute, Wayne, PA. 2012.

40 Rundlöf, T.; Mathiasson, M.; Bekiroglu, S.; Hakkarainen, B.; Bowden, T.; Arvidsson, T. Survey and qualification of internal standards for quantification by 1H NMR spectroscopy, J. Pharm. Biomed. Anal. 2010, 52, 645–651.

41 Calculated by using the formula pD = pH* + 0.4, where pH* is the value measured for H_2O-calibrated pH-meter. (a) C. C. Westcott, pH Measurements; Academic Press: New York, 1978. (b) A. K. Covington, M. Paabo, R. A. Robinson, R. G. Bates, *Anal. Chem.*, 1968, **40**, 700-706.